Exhibit I:

Hunter, C. M., H. Caswell, M. C. Runge, E. V. Regehr, S. C. Amstrup, and I. Stirling. 2007. Polar bears in the Southern Beaufort Sea II: Demography and Population Growth in Relation to Sea Ice Conditions. USGS Science Strategy to Support U.S. Fish and Wildlife Service Polar Bear Listing Decision. U.S. Geological Survey, Reston, Virginia.

USGS
science for a changing world

USGS Science Strategy to Support U.S. Fish and Wildlife Service Polar Bear Listing Decision

Polar Bears in the Southern Beaufort Sea II: Demography and Population Growth in Relation to Sea Ice Conditions

By Christine M. Hunter[1], Hal Caswell[2], Michael C. Runge[3], Eric V. Regehr[4], Steven C. Amstrup[4], and Ian Stirling[5]

Administrative Report

U.S. Department of the Interior
U.S. Geological Survey

U.S. Department of the Interior
DIRK KEMPTHORNE, Secretary

U.S. Geological Survey
Mark D. Myers, Director

U.S. Geological Survey, Reston, Virginia: 2007

Author affiliations:

[1] University of Alaska, Fairbanks
[2] Woods Hole Oceanographic Institution, Massachusetts
[3] U.S. Geological Survey, Patuxent Wildlife Research Center, Maryland
[4] U.S. Geological Survey, Alaska Science Center, Anchorage
[5] Canadian Wildlife Service, Edmonton, Alberta

Contents

List of Figures

List of Tables

Abbreviations, Acronyms, and Symbols

Abbreviations, Acronyms, and Symbols	Meaning
AIC	Akaike's Information Criterion
AR-4	IPCC Fourth Assessment Report
cdf	Cumulative distribution function
COY	Cub-of-the-year
GCM	General circulation models
IPCC	Intergovernmental Panel on Climate Change
IUCN	International Union for Conservation of Nature and Natural Resources
LTRE	Life table response experiment
SB	Southern Beaufort Sea
SRES	Special Report on Emission Scenarios
USFWS	U.S. Fish and Wildlife Service
USGS	U.S. Geological Survey

Polar bears in the southern Beaufort Sea II: Demography and population growth in relation to sea ice conditions

by Christine M. Hunter, Hal Caswell, Michael C. Runge, Eric V. Regehr, Steve C. Amstrup, and Ian Stirling

Abstract

This is a demographic analysis of the southern Beaufort (SB) polar bear population. The analysis uses a female-dominant stage-classified matrix population model in which individuals are classified by age and breeding status. Parameters were estimated from capture-recapture data collected between 2001 and 2006. We focused on measures of long-term population growth rate and on projections of population size over the next 100 years. We obtained these results from both deterministic and stochastic demographic models. Demographic results were related to a measure of sea ice condition, $ice(t)$, defined as the number of ice-free days, in year t, in the region of preferred polar bear habitat. Larger values of *ice* correspond to lower availability of sea ice and longer ice-free periods. Uncertainty in results was quantified using a parametric bootstrap approach that includes both sampling uncertainty and model selection uncertainty.

Deterministic models yielded estimates of population growth rate λ, under low *ice* conditions in 2001–2003, ranging from 1.02 to 1.08. Under high *ice* conditions in 2004–2005, estimates of λ ranged from 0.77 to 0.90. The overall growth rate estimated from a time-invariant model was about 0.997; i.e., a 0.3% decline per year. Population growth rate was most elastic to changes in adult female survival, and an LTRE analysis showed that the decline in λ relative to 2001 conditions was primarily due to reduction in adult female survival, with secondary contributions from reduced breeding probability.

Based on demographic responses, we classified environmental conditions into good (2001–2003) and bad (2004–2005) years, and used this classification to construct stochastic models. In those models, good and bad years occur independently with specified probabilities. We found that the stochastic growth rate declines with an increase in the frequency of bad years. The observed frequency of bad years since 1979 would imply a stochastic growth rate of about -1% per year.

Deterministic population projections over the next century predict serious declines unless conditions typical of 2001–2003 were somehow to be maintained. Stochastic projections predict a high probability of serious declines unless the frequency of bad *ice* years is less than its recent average. To explore future trends in sea ice, we used the output of 10 selected general circulation models (GCMs), forced with "business as usual" greenhouse gas emissions, to predict values of $ice(t)$ until the end of the century. We coupled these to the stochastic demographic model to project population trends under scenarios of future climate change. All GCM models predict a crash in the population within the next century, possibly preceded by a transient population increase.

The parameter estimates on which the demographic models are based have high levels of uncertainty associated with them, but the agreement of results from different statistical model sets, deterministic and stochastic models, and models with and without climate forcing, speaks for the robustness of the conclusions.

1 Introduction

The US Fish and Wildlife Service (USFWS) proposed listing polar bears (*Ursus maritimus*) as a threatened species under the Endangered Species Act in January 2007 (US Fish and Wildlife Service 2007). To help inform their final decision, they requested that the USGS conduct additional analyses of existing data for polar bears and their sea ice habitat. Part of this effort involved demographic analyses to better understand polar bear population status in the southern Beaufort Sea (SB), one of 19 IUCN (International Union for the Conservation of Nature) populations of polar bears worldwide (Aars et al. 2006).

This report addresses demography and projections of population growth for the SB polar bear population in relation to current, recent, and projected environmental conditions in the southern Beaufort Sea. This is part II of a two-part report. Part I (Regehr et al. 2007) includes the details of estimation of the vital rates (survival and breeding probabilities) and describes the biological context of the SB population in relation to the world-wide distribution of polar bears; we will not repeat that information here.

Our goals are to describe the demographic status of polar bears in the SB under current and recent conditions, to describe the effect of sea ice conditions on demography, and to project the future dynamics of the population under a range of future sea ice scenarios. To do this, we develop and analyze both deterministic and stochastic stage-classified matrix population models. Such models are often used as a mathematical framework for studying populations of conservation concern (e.g., Fujiwara and Caswell 2001, Runge et al. 2004, Hunter and Caswell 2005a, Smith et al. 2005, Gervais et al. 2006) because they are flexible enough to be tailored to the biology of the species and the availability of data and have a more completely developed mathematical theory than any other type of population model.

We report measures of potential long-term population growth rate, sensitivity and elasticity of the growth rate to changes in the vital rates, and other demographic statistics that can help provide an understanding of the population response to environmental conditions. We also report the results of short-term population projections, focusing on time scales of 45, 75, and 100 years into the future. Our results are based on estimates of the vital rates obtained under a variety of statistical models, and hence have sampling uncertainty and model selection uncertainty associated with them. One of our goals is to incorporate those sources of uncertainty. This uncertainty is essential to evaluating the risks associated with possible management actions.

2 Demographic model structure

We begin by describing the structure of the model, the estimation of parameters, and the relationship with sea ice conditions.

2.1 The life cycle

Typical of large mammals, polar bears are long-lived, have delayed maturity and low fecundity. Female polar bears in the SB are first available to mate in April-June of their 5th year.[1] Implantation of the conceptus is delayed until September-October when pregnant females enter maternal dens (Derocher and Stirling 1992, Amstrup and Gardner 1994). Females give birth in December-January and nurse until their cubs of the year (COYs) are large enough to leave the den the following March–April (Stirling 1988, Amstrup 2003). Cubs that survive remain with their mothers until they are weaned as 2-year-olds.

We define the overall model structure with a life cycle graph (Figure 1). The model distinguishes 6 female and 4 male stages based on sex, age and reproductive status. Stage 1 and 7 are newly independent 2-year old females and males, respectively. Stages 2 and 3 are females

[1] In this regard, the SB population differs from those in other regions, which typically mate in their 4th year.

aged 3 and 4 years, respectively. Stage 4 is females without dependent young and available to breed (either single or accompanied by 2-year olds). Mothers and their cubs are not independent during the two-plus years of parental care, so we modeled the reproductive stages as mother-cub units. Stage 5 is females accompanied by one or more COYs and stage 6 is females accompanied by one or more yearlings. Males are classified by age; stages 7, 8 and 9 are aged 2, 3, and 4 years, respectively, and stage 10 is males 5 years of age or older. This life cycle graph differs from that used in Regehr et al. (2007) only in that it includes reproduction in addition to the transitions of existing individuals.

The projection interval is from April to April, the time of sampling and when females with COYs typically leave their maternal dens. Transitions of individuals or mother-cub units among stages, and creation of new individuals, are indicated by arcs in the life cycle graph. The transition probabilities of existing individuals are defined in terms of conditional probabilities. The probability that a bear in stage i survives from time t to $t+1$ is $\sigma_i(t)$. The conditional probability that a female in stage i breeds between time t and $t+1$, given survival, is $\beta_i(t)$. The probability that at least one member of a COY litter survives from year t to year $t+1$, given survival of the mother, is σ_{L0}. Thus, for example, the transition from stage 4 to stage 5, which requires a female to survive and breed, occurs with probability $\sigma_4(t)\beta_4(t)$. The transition from stage 4 to stage 4, which occurs when a female survives but does not breed, occurs with probability $\sigma_4(t)(1-\beta_4(t))$.

Fertility in this model appears on the arc from stage 6 to stages 1 (female offspring) and 7 (male offspring). It depends on three quantities: the survival of the mother (σ_6), the survival of at least one member of a yearling litter (σ_{L1}), and the average number of 2-year olds in a successful litter (f). The calculation of σ_{L1} and f is described in Section 2.3.1.

2.2 The demographic model

The life cycle graph corresponds to a stage-structured matrix population model

$$\mathbf{n}(t+1) = \mathbf{A}_t\mathbf{n}(t) \tag{1}$$

where $\mathbf{n}(t)$ is a vector giving the number of individuals in each stage, $n_i(t)$, and $\mathbf{A}_t$ is a population projection matrix that projects the population from t to $t+1$. The entry a_{ij} of $\mathbf{A}$ is the coefficient on the arc from stage j to stage i in the life cycle graph. The projection matrix is given by equation (2).

The upper left 6×6 corner of the matrix describes the production of females by females. The lower right 4×4 corner describes the survival of males. The lower left corner describes the production of males by females.

Polar bears are polygynous and only a portion of females are available to mate in a given year. Therefore, it is unlikely that female fertility is limited by availability of males or fluctuations in the sex ratio. Thus, we expect the growth rate of the population to be determined by the female portion of the life cycle and base all subsequent analyses on the female matrix.

2.3 Parameter estimates

Parameters in the population projection matrix were estimated from a multi-state mark-recapture analysis based on the life cycle graph in Figure 1 (Fujiwara and Caswell 2002, Caswell and Fujiwara 2004). The data consisted of capture histories for 627 polar bears captured in the SB study area between 2001 and 2006 (between Wainwright Alaska and Paulatuk, Northwest Territories, Canada; see Amstrup et al. 1986 and Regehr et al. 2007). We make a few pertinent comments here but details of the parameter estimation can be found in Part I of this report (Regehr et al. 2007).

We used maximum likelihood methods to fit a candidate set of statistical models, developed from biological considerations. The models differed in the extent of age- and stage-specificity of the vital rates and in the dependence of survival and breeding probabilities on time and/or

$$\mathbf{A} = \left(\begin{array}{cccccc|cccc} 0 & 0 & 0 & 0 & 0 & \frac{\sigma_6\sigma_{L1}f}{2} & 0 & 0 & 0 & 0 \\ \sigma_1 & 0 & 0 & 0 & 0 & 0 & 0 & 0 & 0 & 0 \\ 0 & \sigma_2 & 0 & 0 & 0 & 0 & 0 & 0 & 0 & 0 \\ 0 & 0 & \sigma_3 & \sigma_4(1-\beta_4) & \sigma_5(1-\sigma_{L0})(1-\beta_5) & \sigma_6 & 0 & 0 & 0 & 0 \\ 0 & 0 & 0 & \sigma_4\beta_4 & \sigma_5(1-\sigma_{L0})\beta_5 & 0 & 0 & 0 & 0 & 0 \\ 0 & 0 & 0 & 0 & \sigma_5\sigma_{L0} & 0 & 0 & 0 & 0 & 0 \\ \hline 0 & 0 & 0 & 0 & 0 & \frac{\sigma_6\sigma_{L1}f}{2} & 0 & 0 & 0 & 0 \\ 0 & 0 & 0 & 0 & 0 & 0 & \sigma_7 & 0 & 0 & 0 \\ 0 & 0 & 0 & 0 & 0 & 0 & 0 & \sigma_8 & 0 & 0 \\ 0 & 0 & 0 & 0 & 0 & 0 & 0 & 0 & \sigma_9 & \sigma_{10} \end{array}\right) \quad (2)$$

on a covariate describing sea ice conditions (see Section 2.4). Models were evaluated using Akaike's Information Criterion (AIC; Burnham and Anderson 2002). AIC weights were used to produce model-averaged estimates of parameters for three sets of models. We refer to these as the *full model set*, the *non-covariate model set*, and the *time-invariant model set*.

The full model set contained all models with $\Delta AIC \leq 4$. Models in this set described breeding probabilities (β_4, β_5) as time-dependent, survival probabilities (σ_1–σ_6) primarily as covariate dependent, and COY litter survival (σ_{L0}) as either time-invariant, covariate-dependent, or time-dependent.

Covariate dependence was described by a linear function on the logit scale. Because this data set contained only 5 years of recaptures, there was a high degree of uncertainty in the slope and intercept parameters for covariate-dependent survival. Moreover, the results of covariate-dependent models are influenced by the specific functional form of the covariate dependence. To evaluate variation in the vital rates without relying on a particular functional form of covariate-dependence, we used the non-covariate model set, which contained all models with $\Delta AIC \leq 4$ that did not include the covariate (with ΔAIC measured relative to the best model within this set). Comparison of results between the full model set and the non-covariate model set provides a check on robustness of the conclusions from the parametric form of the covariate dependence.

Finally, the time-invariant model set included all models with time-invariant parameters. This set of models represents the best single estimate for the vital rates over the period of the study, although we note at the outset that the data do not support the claim that the rates were, in fact, constant.

Uncertainty in the demographic results arises from sampling variability and model-selection variability of the vital rate estimates. To evaluate this uncertainty, we used a parametric bootstrap procedure that is described in detail in Regehr et al. (2007). Briefly, the method generates B bootstrap samples. Those samples are allocated at random among the models in the model set with probabilities given by the Akaike weights. Within each model, samples of the mathematical parameters $\boldsymbol{\theta}$ are generated from a multivariate normal distribution using the estimated covariance matrix for that model. From each bootstrap set of mathematical parameters, the vital rates $\boldsymbol{\pi}$ are calculated, where $\boldsymbol{\pi}$ contains the stage-specific survival probabilities, breeding probabilities, and fertility. These are used to construct projection matrices and calculate demographic statistics. Unless otherwise noted, we used $B = 10,000$. We present measures of variance either by plotting the distribution of the resulting statistic, or as 90% confidence intervals obtained as the 5th and 95th percentiles of the bootstrap distributions (Efron and Tibshirani 1993).

2.3.1 Fertility

The fertility parameters, σ_{L1} and f, could not be directly estimated by the mark-recapture anal-

ysis, but instead were calculated from the other vital rates and from an independent value for the probability distribution of litter size. The calculation takes account of both survival of individual cubs and the chance of loss of entire litters.

The size distribution of a litter (of COYs) in stage 5 was set to

$$\mathbf{c} = \begin{pmatrix} 0.276 & 0.724 \end{pmatrix} \tag{3}$$

where c_i is the probability of a litter of size i. These values were obtained from capture data collected in 2001–2006 in the SB management unit. We included only one- and two-cub litters because triplets are rare for polar bears inhabiting the Arctic basin (Amstrup 2003). We did not investigate variation in this parameter.

The probability of loss of a COY litter is

$$1 - \sigma_{L0} = (1-s)c_1 + (1-s)^2 c_2 \tag{4}$$

where s is a measure of survival of a COY. That is, a COY litter is lost if it consists of one cub which dies, or two cubs both of which die. Given $\mathbf{c}$ and an estimate of σ_{L0}, we solve (4) for s.

Conditional on not losing the COY litter, the size distribution of a yearling (stage 6) litter is

$$y_1 = [c_1 s + 2c_2 s(1-s)]/\sigma_{L0} \tag{5}$$
$$y_2 = c_2 s^2/\sigma_{L0} \tag{6}$$

The probability of loss of the yearling litter between stage 6 and stage 1 is then

$$1 - \sigma_{L1} = (1-\sigma_1)y_1 + (1-\sigma_1)^2 y_2 \tag{7}$$

where we assume that the survival of a yearling cub is the same as that of a 2-year old bear in stage 1. Conditional on not losing the yearling litter, the size distribution of the litter arriving at stage 1 is then

$$z_1 = [y_1\sigma_1 + 2y_2\sigma_1(1-\sigma_1)]/\sigma_{L1} \tag{8}$$
$$z_2 = \left[y_2\sigma_1^2\right]/\sigma_{L1} \tag{9}$$

The expected number of new stage 1 bears, conditional on not losing the yearling litter, is then

$$f = z_1 + 2z_2. \tag{10}$$

Multiplying this by the survival of the mother and the probability of not losing the litter, and dividing by 2 to account for the sex ratio, gives the fertility $\sigma_6\sigma_{L1}f/2$.

2.4 Climate model projections

The SB region is covered with annual sea ice from approximately October to June, and partially or completely ice free from July to September, when sea ice retreats northward into the Arctic basin (Comiso 2006, Richter-Menge et al. 2006). To represent ice conditions and habitat availability for polar bears we derived an index of sea ice conditions. This index, $ice(t)$, was the number of days during calendar year t that were ice-free in the region of preferred habitat for polar bears. Preferred habitat was defined as waters within the SB management unit east of Barrow, AK, with an ocean depth less than 300 m because polar bears in the SB select strongly for sea ice over the shallow waters of the continental shelf (Durner et al. 2004, 2007). A day was considered ice free if the mean ice concentration in preferred habitat area was less than 50%. Mean ice concentration was the arithmetic mean of daily ice concentration values for the 139 grid cells (25×25 km) in the preferred habitat area based on passive microwave satellite imagery (from the National Snow and Ice Data Center, Boulder, Colorado, USA; `ftp://sidads.colorado.edu/pub/`). Regehr et al. (2007) found that the *ice* covariate was highly negatively correlated with the availability of polar bear habitat as described by resource selection functions (Durner et al. 2007)

Larger values of *ice* correspond to longer ice-free periods and reduced amounts of ice available to polar bears. So we expect the effect on survival, breeding, and population growth to be negative. The multistate mark-recapture analysis (Regehr et al. 2007) found evidence of such negative effects, using models in which the relationship between survival probabilities and *ice* was described using a logistic function; i.e.,

$$\text{logit}\left[\sigma_i(t)\right] = a_i + b_i\, ice(t). \tag{11}$$

2.5 Demographic analysis sequence

A matrix population model (1) can assume several forms, depending on whether the entries in **A** are time-invariant, time-dependent, or dependent on an environmental covariate. In what follows, we analyze deterministic models, which assume that environmental conditions remain constant over time, and stochastic models, which allow for variation in environmental conditions. By analyzing a sequence of models we are able to obtain more robust conclusions than would be possible from examining any single model. To orient the reader we give an outline here of the sequence of models and analyses. The models we focus on are

1. Deterministic models
   (a) time-invariant
   (b) year-specific
2. Stochastic models
   (a) stationary stochastic environments
   (b) climate model scenarios

We begin with deterministic models. The simplest of these is time-invariant, in which the projection matrix is obtained from a single estimate of the vital rates over the entire period 2001–2005. Then we consider year-specific models, in which a separate projection matrix is obtained for each of the years 2001,. . . ,2005. The calculations from a given year-specific matrix give the population dynamics that would result if the conditions in that year were maintained indefinitely.

Then we incorporate environmental variation by constructing stochastic models. We classify these by the way the environment is described. The simplest model is obtained by describing the environment as a stationary process, i.e., one which fluctuates, but whose mean, variance, and other statistical properties do not change with time. In our models, the stationary stochastic environment is characterized by the frequency of years with poor sea ice conditions (in a sense to be described precisely below). Rather than assuming a stationary stochastic environment, our second set of models derives a stochastic environment from the output of general circulation models (GCMs) for climate over the next century. These models are nonstationary, because they not only fluctuate, but their statistical properties change over time.

The deterministic year-specific calculations show the consequences of the conditions in the years in which the parameters were estimated. The stochastic models use that information to project the consequences of future environmental fluctuations. Because the stochastic models use the year-specific models as components, it is important to understand the behavior of the deterministic models. For both deterministic and stochastic calculations we compare the results of models parameterized from the full model set, the non-covariate model set, and for deterministic models the time-invariant model set. For all except the climate model scenarios, we examine both long-term population growth rates and short-term projections of population size.

As was emphasized in Part I of this report (Regehr et al. 2007), estimating the vital rates from the available data was subject to large degrees of sampling and model selection uncertainty. Examining multiple models helps document the robustness, or lack thereof, of the conclusions, as we discuss in Section 5.

3 Deterministic demography

We begin with the analysis of deterministic versions of the demographic model.

3.1 Deterministic methods

We apply deterministic demographic analyses to the time-invariant model set, the full model set, and the non-covariate model set. In most cases, and unless otherwise specified, results for the full model set and the non-covariate model set were very similar.

The full model set and the non-covariate model set contain year-specific parameter estimates. As a result, demographic quantities calculated from them are also year-specific, in the

following sense. Suppose we take the vital rates for 2001, construct the projection matrix $\mathbf{A}$, and calculate a population growth rate. That rate describes the long-term population growth that would occur if the conditions in 2001 were held constant. Thus the growth rate represents, and summarizes, the conditions present in 2001, by asking what would happen if they were to be maintained. Such results are called projections, to distinguish them from predictions, or forecasts, that attempt to say what will actually happen in the future.

We calculate the long-term population growth rate as the dominant eigenvalue λ of $\mathbf{A}$. The continuous-time growth rate r is given by $r = \log\lambda$. If $\lambda > 1$ (i.e., $r = \log\lambda > 0$) the population will increase if the conditions remain the same. If $\lambda < 1$ (i.e., $r = \log\lambda < 0$) the population will decline to extinction unless conditions change. Under constant conditions, the population will eventually converge to a stable stage structure proportional to the right eigenvector $\mathbf{w}$ corresponding to λ. The left eigenvector $\mathbf{v}$ corresponding to λ gives the distribution of reproductive values among the stages. A population that is not at the stable stage distribution will go through a period of transient fluctuations in both abundance and structure before the asymptotic growth rate is realized. These transient fluctuations can be analyzed in terms of the subdominant eigenvalues and eigenvectors of $\mathbf{A}$, or revealed by short-term projections (see Section 3.1.3).

3.1.1 Perturbation analysis

Perturbation analysis measures the effect on population growth of changes in parameters. The sensitivity of population growth rate to a parameter is the absolute change in population growth rate caused by a small absolute change in a parameter. The sensitivity of λ to a parameter π is

$$\frac{\partial\lambda}{\partial\pi} = \mathbf{v}^{\mathsf{T}}\frac{\partial\mathbf{A}}{\partial\pi}\mathbf{w} \tag{12}$$

where the eigenvectors are scaled so that their scalar product $\langle\mathbf{v},\mathbf{s}\rangle = 1$ (Caswell 1978, 2001) and the derivative $\partial\mathbf{A}/\partial\pi$ is a matrix whose (i,j) entry is $\partial a_{ij}/\partial\pi$. If $\pi = a_{ij}$, then (12) reduces to

$$\frac{\partial\lambda}{\partial a_{ij}} = v_i w_j. \tag{13}$$

It is often useful to express changes in parameters, and their effects, on a proportional scale. The elasticity of population growth rate to a parameter is the proportional change in population growth rate caused by a proportional change in the parameter, and is given by

$$\frac{\pi}{\lambda}\frac{\partial\lambda}{\partial\pi}. \tag{14}$$

3.1.2 LTRE analysis

Differences in population growth rate λ among years are the integrated result of all the differences in stage-specific survival, transitions, and reproduction among those years. LTRE (life table response experiment) analyses decompose those differences into contributions from the difference in each of the vital rates (Caswell 1989, 2001).

Let π_i be one of the demographic parameters (survival probability, litter survival, breeding, f, or σ_{L1}). We choose the conditions in 2001 as our reference, and examine the changes in λ relative to this. Let λ_r be the growth rate under the reference conditions and λ_t be the growth rate under conditions in year t. Then, to first order,

$$\lambda_t - \lambda_r \approx \sum_i \left(\pi_i^{(t)} - \pi_i^{(r)}\right) \left.\frac{\partial\lambda}{\partial\pi_i}\right|_{\frac{\pi_i+\pi_r}{2}}. \tag{15}$$

The sensitivity term is calculated at the mean of the reference and the treatment parameters. The ith term in the summation on the right hand side is the contribution of the differences in the parameter π_i to the difference in λ. A parameter may make a small contribution if it does not differ much, or if λ is not very sensitive to differences in that parameter.

3.1.3 Population projection

Population growth rate λ gives the long-term rate of population growth. In the short-term,

growth may fluctuate because of deviations from the stable stage distribution. To evaluate this, we projected population growth for 45, 75, and 100 years[2] according to (1), starting from an initial population proportional to

$$\mathbf{n}(0) = \begin{pmatrix} 0.106 & 0.068 & 0.106 & 0.461 \\ & & 0.151 & 0.108 \end{pmatrix}^{\mathsf{T}}. \quad (16)$$

This is an estimate of the structure of the SB population, averaged over 2004–2006. It is obtained from a Horvitz-Thomson estimator applied to mark-recapture data in the SB population using recapture probabilities from Regehr et al. (2006).

Because the models under consideration here are linear, the projections produce population size measured relative to the initial population, and thus can be directly interpreted in terms of proportional increase or decrease. Bootstrap samples were used to document the uncertainty in projected population size for each model set.

3.1.4 Correction for harvest mortality

Polar bears in the SB management unit are harvested as part of annual regulated hunts by native user groups in the US and Canada (Brower et al. 2002). Regehr et al. (2007) used tag return data to estimate a harvest component h of total mortality for female bears in stages 1–4. To find the survival rate in the absence of harvest, we removed the current level of harvest from the estimated survival rates by replacing σ_i with $\frac{\sigma_i}{(1-h)}$. To evaluate the effect of various rates of harvest mortality on population growth rate, we then applied a range of harvest rates up to 0.1 to stages 1–4. Harvest mortality was not considered for stages 5 and 6 because hunters are discouraged from taking females with dependent cubs.

3.2 Results of deterministic analysis

3.2.1 Growth rates

Population growth rates are summarized in Table 1. The time-invariant model set predicts a growth rate very close to stationarity ($\lambda = 0.997$, implying a decline of -0.3% per year). The full model set and the non-covariate model set both predict population growth or stability under the conditions in 2001–2003 and population decline under the conditions in 2004–2005. The estimates of population growth rate are accompanied by significant uncertainty (Figure 2). However, in 2004–2005, with a longer ice-free season, only a tiny percentage of the bootstrap samples produced positive population growth.

The stable stage distribution contains more individuals in the adult stages than in sub-adult stages. (Figure 3). In years with a longer ice-free season the proportion of individuals in the adult but not reproducing stage increased and the proportion in all other stages decreased, particularly the reproducing stages (Figure 3). However, the distribution of individuals among the six stages was not qualitatively different. Similarly, the reproductive value of reproducing stages increased in years with poor conditions but this change was relatively small (not shown).

In long-lived species, the sensitivity and elasticity of population growth rate to model parameters is typically greatest for adult survival rates (e.g., Heppell et al. 2000). This population was no exception, with λ most sensitive and most elastic to survival of the adult female stages (σ_4–σ_6). See Figure 3 for the full model set and Figure A-2 for the non-covariate model set.. Among the other parameters, only the breeding probability of an adult female without cubs (β_4) makes a significant contribution to population growth rate. Under the conditions of 2004–2005, the sensitivity and elasticity of λ to survival of individuals in stage 4 (adult, not currently reproducing) increased. This partly reflects the increase in the proportion of individuals in this stage under these conditions, which increases its importance to λ.

The LTRE analysis decomposes the differences in λ (measured relative to 2001 conditions) into contributions from each of the vital rates. The decline in λ is mostly due to declines in adult survival in stages 4–6 (σ_4, σ_5, and σ_6), with secondary contributions from the breeding

[2]The 45-year projection horizon was specifically requested by the FWS.

probability of females in stage 4 (β_4) (Figures 4).

3.2.2 Deterministic population projections

Short-term projections of the population show that exponential growth is achieved quickly when constant conditions are maintained; with no apparent transient effects (Figure 5). This is expected because the initial population vector (16), based on current population estimates, is not far from the stable stage distribution.

The uncertainty in the short-term projections is shown by the probability distribution, over the bootstrap sample, of the log of total female population size at 45 years relative to the starting population size, i.e. $log\left(\frac{N(45)}{N(0)}\right)$. Under the conditions experienced in years 2001–2003, a high proportion of the bootstrap samples yield population increase. Under the conditions of 2004–2005, almost all the boostrap samples yield population decline, often to very low values (Figures 5, A-3, and A-4).

Figure 5 shows the cumulative distribution function (cdf) for this relative growth (the cumulative distribution at x is the probability that the variable in question is less than or equal to x). Most of the mass for the cdf's in 2001–2003, is gained to the right of the zero line, indicating that most of the probability distribution produces positive population change. The cdf's for conditions in 2004 and 2005 approach 1 to the left of the zero line, indicating that almost all of the probability distribution predicts population decline. The distributions in Figure 5 reflect the distribution of population growth rates in Figure 2. Projections to 75 or 100 years merely extend the patterns apparent at 45 years (Figure A-4).

The differences among years in the results of population projection is partly due to vital rates expressed as functions of the *ice* covariate. As noted above and in Regehr et al. (2007), estimating dependence on *ice* was difficult because the capture-recapture data set spanned only five years, so we also examined non-covariate models. Figure 6 compares the population growth rate λ predicted by the full model set as a function of *ice* with the values of λ estimated from the non-covariate model set. The similarity is remarkable.

From this figure, it appears that values of *ice* greater than approximately 125 ice-free days per year lead to precipitous declines in λ, but that below this level λ is relatively insensitive to *ice*. Of course, the pattern of λ for values of *ice* greater than those observed in the data is an extrapolation that depends completely on the parametric form (logistic) assumed for the covariate-dependence. This range of values could be explored only through continued capture-recapture studies of the SB population.

3.2.3 Effects of harvest

The effects of the harvest level of females on population growth rate λ are shown in Figure 7; the level of female harvest to which the population is currently subject has only a small effect on population growth rate.

4 Stochastic demography

Environmental conditions have changed over the course of this study, and will no doubt change in the future. The deterministic analyses (Section 3.2) characterize those conditions by projecting the population growth patterns that would result if the conditions were somehow kept constant. Now we turn to the effects of the fluctuations themselves, using stochastic models.

A stochastic demographic model contains a model of the environment, a link from the environment to the vital rates, and a projection of the population using those vital rates. We will present results of two stochastic calculations, which differ in the scenarios used to describe variation in the environment.

Based on the patterns in survival (Regehr et al. 2007) and in population growth rate λ (Table 1, Figure 6), we classified 2001–2003 as "good" years, characterized by high survival and estimates of population growth rate λ greater than 1. We classified 2004–2005 as "bad" years, characterized by reduced survival, and values

of λ much less than 1. Our first approach to stochastic models is based on the statistical patterns of good and bad years.

Good years are associated with low values of *ice*, and bad years are characterized by high values of *ice*, but our first analysis does not make any explicit connection to the dynamics of ice. Instead, it assumes that good and bad years occur independently and with a constant probability q of a bad year and $1-q$ of a good year. Population growth in such a stochastic environment will depend on the value of q (i.e., on the long-term frequency of bad years), and we examine this dependence. Although the environment fluctuates, its statistical properties (e.g., the value of q) do not, so we call this a stationary stochastic environment.[3]

Our second approach explicitly links the vital rates to future sea ice conditions. We used the output of a set of 10 IPCC (Intergovernmental Panel on Climate Change) climate models (DeWeaver 2007 describes the choice of these models) to forecast scenarios of sea ice conditions until the year 2100. We used the output from these climate models to generate stochastic sequences of good and bad years, and used those sequences to project polar bear population size through the end of the century.

Stochastic calculations include several different kinds of uncertainty. They include uncertainty due to environmental stochasticity: even if the probability of a bad year is fixed, sometimes a bad year will occur and sometimes it will not. They include uncertainty due to the sampling error in the vital rates, which we assess using bootstrap samples and by comparing the full and non-covariate model sets. Finally, they include uncertainty due to the uncertainty in forecasts of future climate conditions. We obtain some information on this uncertainty by using 10 climate models rather than a single model, but it is not possible to examine climate forecast uncertainty within a single climate model because multiple stochastic realizations of climate model output are generally not available.

[3]Mathematically speaking, it is a particularly simple type of stationary environment, in which successive states of the environment are independently and identically distributed.

4.1 Stochastic methods

In this section we describe the methods used for stochastic calculations.

4.1.1 Stationary stochastic environments

Let $\mathbf{A}^{(1)}, \ldots \mathbf{A}^{(5)}$ denote the projection matrices, for females, estimated in years 2001–2005, and let q be the probability of occurrence of a bad year. In a bad year, the population experiences a matrix chosen from the set $\{\mathbf{A}^{(4)}, \mathbf{A}^{(5)}\}$ with probability 1/2. In a good year, the population experiences a matrix chosen from the set $\{\mathbf{A}^{(1)}, \mathbf{A}^{(2)}, \mathbf{A}^{(3)}\}$ with probability 1/3. Thus the population grows according to

$$\mathbf{n}(t+1) = \mathbf{A}_t \mathbf{n}(t) \tag{17}$$

where the matrix $\mathbf{A}_t$ is

$$\mathbf{A}_t = \begin{cases} \mathbf{A}^{(1)} & \text{with probability } (1-q)/3 \\ \mathbf{A}^{(2)} & \text{with probability } (1-q)/3 \\ \mathbf{A}^{(3)} & \text{with probability } (1-q)/3 \\ \mathbf{A}^{(4)} & \text{with probability } q/2 \\ \mathbf{A}^{(5)} & \text{with probability } q/2 \end{cases} \tag{18}$$

This algorithm uses the variability within the good years, and within the bad years, as estimates — admittedly crude but better than nothing — of the variation in the vital rates within these categories (see Caswell and Kaye 2001 for another example).

Because this environmental process is stationary and ergodic, and because the projection matrices form an ergodic set (e.g., Tuljapurkar 1990), the population has an expected per-year growth rate given by

$$\log \lambda_s = \lim_{T\to\infty} \frac{1}{T} \log \|\mathbf{A}_{T-1} \cdots \mathbf{A}_0 \mathbf{n}_0\| \tag{19}$$

where $\|\cdot\|$ is the 1-norm and $\mathbf{n}_0$ is an arbitrary initial population vector.

This growth rate is the stochastic analog of the population growth rate λ in a time-invariant environment, and is thus the relevant measure

of long-term population growth in a stochastic environment. If $\log \lambda_s \leq 0$, the population will eventually decline to extinction (unless something happens to change the environment or the vital rates). If $\log \lambda_s > 0$ the population will eventually grow, but even so, stochastic fluctuations may carry it to sufficiently low densities to cause extinction.

We estimated $\log \lambda_s$ by applying (19) with $T = 5000$. The effects of parameter uncertainty were evaluated by repeating these calculations for 2000 samples from the parametric bootstrap distribution of the vital rates.

The stochastic growth rate is an asymptotic (long-term) index of population growth, as is λ in the deterministic model. Thus we also carried out short-term projections, starting with an initial population with the observed population structure (16), and calculated the proportional increase or decrease in total population size at times $t = 45, 75$, and 100 years.

4.1.2 Sensitivity analysis of the stochastic growth rate

To calculate the sensitivity of $\log \lambda_s$ and the elasticity of λ_s to changes in parameters, we used the perturbation analysis of Tuljapurkar (1990) and Caswell (2005, 2007).

Following Regehr et al. (2007), let $\boldsymbol{\pi}$ be the vector of demographic parameters

$$\boldsymbol{\pi} = \begin{pmatrix} \sigma_1 & \cdots & \sigma_6 & \sigma_{L0} & \beta_4 & \beta_5 & f \end{pmatrix}^{\mathsf{T}} \quad (20)$$

and let

$$\frac{d \log \lambda_s}{d \boldsymbol{\pi}^{\mathsf{T}}} = \begin{pmatrix} \frac{d \log \lambda_s}{d \pi_i} \end{pmatrix} \quad (21)$$

be the 1×10 vector of the sensitivities of $\log \lambda_s$. To calculate these sensitivities, we generate a random sequence of matrices $\mathbf{A}_t$ for $t = 0, \ldots, T-1$. We use this sequence to generate a sequence of stage distribution vectors

$$\mathbf{w}(t+1) = \frac{\mathbf{A}_t \mathbf{w}(t)}{\|\mathbf{A}_t \mathbf{w}(t)\|}, \qquad t = 0, \ldots, T-1, \quad (22)$$

one-step growth rates

$$R_t = \|\mathbf{A}_t \mathbf{w}(t)\|, \quad (23)$$

and reproductive value vectors

$$\mathbf{v}^{\mathsf{T}}(t-1) = \frac{\mathbf{v}^{\mathsf{T}}(t)\mathbf{A}_{t-1}}{\|\mathbf{v}^{\mathsf{T}}(t)\mathbf{A}_{t-1}\|} \qquad t = 1, \ldots, T. \quad (24)$$

In these calculations, the starting vectors $\mathbf{w}(0)$ and $\mathbf{v}(T)$ are arbitrary non-zero, non-negative vectors with $\|\mathbf{w}(0)\| = \|\mathbf{v}(T)\| = 1$. Then the sensitivities are calculated as

$$\frac{d \log \lambda_s}{d \boldsymbol{\pi}^{\mathsf{T}}} = \lim_{T \to \infty} \frac{1}{T} \sum_{i=0}^{T-1} \frac{\left[\mathbf{w}^{\mathsf{T}}(i) \otimes \mathbf{v}^{\mathsf{T}}(i+1)\right]}{R_i \mathbf{v}^{\mathsf{T}}(i+1)\mathbf{w}(i+1)} \times \left(\frac{d \mathrm{vec}\, \mathbf{A}_i}{d \boldsymbol{\pi}^{\mathsf{T}}} \right). \quad (25)$$

The elasticity of λ_s is

$$\lim_{T \to \infty} \frac{1}{T} \sum_{i=0}^{T-1} \frac{\left[\mathbf{w}^{\mathsf{T}}(i) \otimes \mathbf{v}^{\mathsf{T}}(i+1)\right]}{R_i \mathbf{v}^{\mathsf{T}}(i+1)\mathbf{w}(i+1)} \times \left(\frac{d \mathrm{vec}\, \mathbf{A}_i}{d \boldsymbol{\pi}^{\mathsf{T}}} \right) \mathrm{diag}\,(\boldsymbol{\pi}_i). \quad (26)$$

In these expressions, $\otimes$ denotes the Kronecker product, and $d\mathrm{vec}\, \mathbf{A}_i / d\boldsymbol{\pi}^{\mathsf{T}}$ is the matrix (dimension 36×10) of derivatives of the entries of $\mathbf{A}_i$ with respect to the parameters in $\boldsymbol{\pi}$. We calculated all sensitivities and elasticities using $T = 5000$.

4.1.3 Climate model scenarios

To project population growth under future climate change scenarios, we extracted forecasts of the availability of sea ice for polar bears in the SB region, using monthly forecasts of sea ice concentration from 10 IPCC Fourth Assessment Report (AR-4) fully-coupled general circulation models (GCMs; Table 2; see DeWeaver 2007 for details of the selection process and properties of the models). We used forecasts for the 21st century based on a "business as usual" greenhouse gas forcing scenario (Special Report on Emission Scenarios SRES-A1B). The 10 GCMs were selected based on concordance between their 20th century simulations (20c3m) of sea ice extent and the observational record of ice extent during 1953–1995 (DeWeaver 2007).

Because GCMs do not provide suitable forecasts for areas as small as the SB, we used sea ice concentration for a larger area composed of 5 IUCN polar bear management units (Aars et al. 2006) with ice dynamics similar to the SB management unit (Barents Sea, Beaufort Sea, Chukchi Sea, Kara Sea and Laptev Sea; see Rigor and Wallace 2004, Durner et al. 2007). We assumed that the general trend in sea ice availability in these 5 units was representative of the general trend in the Southern Beaufort region.

From each GCM output we calculated the number of ice-free months during the calendar year in the region of preferred habitat for polar bears within the 5 IUCN units. Preferred habitat was defined as waters over the continental shelf and less than 300m deep (International Bathymetric Chart of the Arctic Ocean; http://www.ngdc.noaa.gov/mgg/bathymetry /arctic/arctic.html). A month was considered ice-free if the mean ice concentration in this region was less than 50%. Mean ice concentration was the arithmetic mean ice concentration for all grid cells in the region of preferred habitat. Among the 10 GCMs analyzed, the sea ice grids had model-specific spatial resolutions ranging from 1×1 to 3×4 degrees of latitude and longitude (DeWeaver 2007).

We transformed the ice-free months to ice-free days by multiplying by 30. Then the output of each GCM was shifted so that the projected 2005 value coincided with the mean (114.4 days) of the ice-free days observed in the SB during 2000–2005. This calibrated all the models and produced sea ice projections scaled relative to the observed current (or recent past) conditions. Each year in the shifted trajectory was then classified as good or bad depending on whether the number of ice-free days was greater than or less than 127 (a value midway between the values observed during the good years 2001–2003 and the bad years 2004–2005). To extract trends in the frequency of bad years from this binary series, we applied a Gaussian kernel smoother as described by Copas (1983; see Smith et al. 2005 for an ecological application similar to this one). The kernel standard deviation (2.5 years) was chosen, as suggested by Copas (1983), as a subjective compromise between smoothing and variation.

Because these are short-term projections and because the stochastic properties of the environment change, there is no single measure of population growth. Instead, we projected the population from 2005 to 2100, with $\mathbf{n}(0)$ given by (16), and with a matrix $\mathbf{A}_t$ chosen randomly at each year with probabilities (18), with q as the probability of a bad year in year t. The proportional increase or decrease in total population size was recorded for each year.

4.2 Results of stochastic analysis

4.2.1 Stationary stochastic environments

Population growth rates. The stochastic growth rate declines with increases in the frequency of bad years, shown in Figure 8. The results for the full model set have been partitioned into two subsets because of an unexpected (and pathological) behavior of the these models with ice-covariate dependence. Because of the high variance in, and strong negative correlation between, the estimates of the slope and intercept of this response, a fraction (about 11%) of the bootstrap samples showed a *positive* response to bad ice years. Because of the behavior of the logistic function, these led to extremely negative population growth rates under conditions of good ice years ($\log \lambda_s$ as low -20, which corresponds to a population half-life of 12 days). Neither a positive response to ice-free conditions nor a population half-life measured in days are biologically realistic, so we have partitioned the bootstrap samples of the full model set into a subset conditional on a non-increasing response and an (unrealistic) subset conditional on an increasing response, and we focus on the non-increasing subset. However, this partition obviously affects our conclusions about trends, so we rely on comparison with the non-covariate set of models, which is not partitioned in any way.

In both sets of models, the stochastic growth

rate decreases nearly linearly with increases in the frequency q of bad years. The slope implies that an increase of 0.1 in q would reduce the stochastic growth rate $\log \lambda_s$ by 0.02y^{-1} (non-covariate model set) or 0.03y^{-1} (full model set). There is a critical threshold frequency above which $\log \lambda_s < 0$ and the population will decline; this is $q \approx 0.175$ (non-covariate model set) or $q \approx 0.165$ (full model set). These estimates of the critical frequency should be compared to the average frequency of bad ice years observed since 1979 ($6/28 = 0.21$), with an apparent increasing trend and decadal oscillations (Figure 9). This observed frequency implies a stochastic growth rate on the order of -0.014 for the full model set and -0.007 for the non-covariate model set.

The elasticity of the stochastic growth rate λ_s to changes in parameters is shown in Figure 10 for the full model set and Figure A-5 for the non-covariate model set, for a range of frequencies (q) of bad years. Regardless of q, the stochastic growth rate is most affected by changes in adult female survival, in a pattern similar to that of the deterministic growth rate (Figure 3).

Population projection. The distributions of relative population size at $t = 45$, 75, and 100 are shown in Figure 11. When bad years are very rare ($q = 0.01$), the probability of decline is approximately 0.25 for the non-covariate model set and 0.20 for the full model set. When $q = 0.25$ (similar to the observed average frequency of bad ice years since 1979), the probability of decline at 45 years is approximately 0.6 for the non-covariate set and 0.9 for the full model set. Decline to a population only 1% of its current size might be considered a severe decline; it would certainly put the population at risk of extinction. With $q = 0.25$, the probability of such a decline within 45 years is approximately 0.2 for either model set.

Extending the time horizon increases the risk of extreme decline. With $q = 0.25$, as t increase from 45 to 75 to 100 years, probability of extreme decline (to 1% of initial size) increases from about 0.2 to 0.4 to 0.55 for the full model set. The corresponding probabilities from the non-covariate model set are about 0.15, 0.2, and 0.25 (Figure 11).

4.2.2 Climate model projections

Figure 12 (top panel) shows the coarse-grained outputs of the climate models (integer values of ice-free months). The 10 models differ in their trends and intercepts, but they all predict increases over the next century. Figure 12 shows the results of rescaling these projections (middle panel) and transforming the trends into the predicted probability of bad ice conditions (bottom panel). Figure A-6 displays these trends for each model individually. All 10 of the climate models agree in forecasting an increase in the incidence of bad years, reaching an incidence of 1 within the next century; indeed, all but one of the models makes this prediction within the next 50 years. Two GCMs (miub_echo_g and mpi_echam5) differ from the rest in predicting a long delay (20–40 years) before the probability of a bad ice year rises above zero.

Figure 13 shows population trajectories sampled from the bootstrap distribution of matrices and the 10 climate models. Most trajectories decline to very low values well before the end of the century. A few outliers increase greatly before declining. Closer examination (Figures A-7 and A-8) reveals that these are associated with the two GCMs that predict no bad years for the next several decades.

The declines shown in Figure 13 obviously carry some risk of extinction. However, the models we use here can project population size as declining exponentially towards zero, but can never actually reach zero. Thus any interpretation in terms of extinction must be accompanied by a definition of an extinction threshold.[4] If the current SB population numbers about 1500 individuals (Regehr et al. 2006),

[4]Such thresholds are often called quasi-extinction thresholds, to distinguish them from true extinction. They may represent values believed to result in real extinction, or simply thresholds felt to be of management concern.

then a decline to 0.001 of current size corresponds to a population of 1.5 bears, almost certainly incompatible with persistence. A decline to 0.01 of current size corresponds to 15 bears, which would certainly be at a high risk of extinction. Figure 14 shows the risk of declining to the thresholds of 0.01 and 0.001, treating the sampled set of population trajectories as a probability distribution measuring our uncertainty about future dynamics. The risk of quasi-extinction, under either threshold and from either model set, exceeds 75% by the end of the century.

5 Discussion

We developed models for the current and future demography of polar bears in the southern Beaufort Sea that link sea ice conditions to population dynamics, embedding the parameter estimation directly in the modeling effort and taking full account of uncertainty that derives from a number of sources. We were able to make use of state-of-the-art demographic methods, coupling them with results from GCM models. This work is an important new analysis of the status of the polar bear population in this region, and is also one of the first efforts to integrate demographic and climate models. Below, we discuss the results, their importance, and considerations in the interpretation of our conclusions.

5.1 Interpretation of results

In this study, we were challenged to provide demographic analyses of a long-lived species living in a highly dynamic environment which is undergoing dramatic changes, and to do so on the basis of a relatively short-term set of estimates of the vital rates. We have also been charged with going beyond characterizing current conditions to projecting the results of future scenarios.

Neither of these are easy tasks, which explains our continual invocation of results from multiple sets of statistical models, from both deterministic and stochastic demographic models, from stochastic models that do and that do not rely on GCMs for future sea ice scenarios, and from 10 different GCM projections. This, unfortunately, may leave the reader lost in a blizzard of detail. So, here we discuss and interpret the overall results.

The reduction in survival and breeding probabilities documented in Part I of this report (Regehr et al. 2007) translate into declines in the population growth rate λ from 2001 to 2005. An LTRE analysis, which decomposes the difference in λ into contributions from the vital rates, shows that the decline in λ is due primarily to reductions in adult female survival, and secondarily to reductions in breeding probability.

Projecting population size using the year-specific vital rates gives increases under the conditions in 2001–2003, but decreases under the conditions of 2004–2005. The interpretation of these results is clear: the SB environment declined in quality (as far as polar bear populations are concerned) over the study period to a point where, if nothing changes, the population will decline rapidly to extinction.

Of course, things do change, and our stochastic analyses address these changes. We phrase these results in terms of good and bad years. It is important to understand these categories. There was a qualitative difference in the potential for population growth between the conditions of 2001–2003 and of 2004–2005. This difference was associated with an approximately 50% increase in the duration of the ice-free period (as measured by the ecologically-motivated covariate *ice*). Our division of the years 2001–2005 into good and bad is not based on a priori ideas of the effects of ice, but on the basis of the population response to those conditions. It is an admittedly crude binary classification of a much more complicated response. Continuation of capture-recapture studies in the SB would make it possible to refine this description of the effects of the environment.

Even so, at this level of resolution it is clear that the frequency of bad years in the future will determine the fate of the SB polar bear popula-

tion. A frequency greater than about 0.17 (one bad year in 6) will produce a negative stochastic growth rate and (unless something changes) lead to eventual extinction. The observed frequency of bad years appears to have been increasing since records began in 1979 (Figure 9),[5] but even taking the average observed frequency (0.21) predicts a population decline of about 1% per year.

This prediction is not far from the deterministic growth rate calculated from a time-invariant model. It would be useful to have independent data on recent trends in size of the SB population to corroborate these results, but such information is not available. However, Amstrup et al. (1986) estimated an approximate population size of $N \approx 1800$ in the mid-1980s and Regehr et al. (2006) estimated a population size of approximately 1500 in 2006. A decrease from $N = 1800$ to $N = 1500$ between 1986 and 2006 represents an average decline of 0.9% per year. Anecdotal evidence suggests that the population may have increased slightly from its mid-1980s level into the 1990s (Amstrup et al. 2001). If the decline from 1800 to 1500 took place over 15 years, it would represent a rate of 1.2% per year, over 10 years, a decline at a rate of 1.8% per year. Such comparisons are difficult because of the scant independent historical data and a high degree of uncertainty around historical population estimates. Nevertheless, the comparison supports our estimates, to the extent that such limited data can provide support.

No one, of course, predicts that Arctic sea ice conditions will be stationary (e.g., IPCC 2007, Overland and Wang 2007, Stroeve et al. 2007). Our projections of future population dynamics based on sea ice forecasts from 10 GCMs all show polar bear populations crashing within the next century. The probability of quasi-extinction, with thresholds of 0.01 or 0.001 (1% or 0.1% of current size) exceeds 0.7. The details, but not the outcome, are sensitive to the choice of GCM (see especially Figures A-7 and A-8).

The links between loss of sea ice and survival, reproduction, and population growth could be simple or complex. Sea ice retreat forcing polar bears to swim longer distances, thus increasing the risk of drowning or starvation, would be a fairly simple connection between increased open water and survival. However, a reduction in the duration of ice cover over water depths less than 300m will also affect many ice-dependent species such as ringed seals (*Phoca hispida*), bearded seals (*Erignathus barbatus*), and arctic cod (*Boreogadus saida*); see e.g. Gaston et al. (2005). Many food web links may be involved in these effects. Intuitively, reduction in the availability of ringed seals, a primary prey species of polar bears, whose preferred habitat is ice over waters less than 300 m depth (Stirling et al. 1982), must play a role.

The formal spatial scope of inference for this work is the southern Beaufort Sea population, but to the extent that the SB represents other populations in the divergent polar basin (Amstrup et al. 2007), inference could be applied to this larger zone. The *ice* covariate was calculated from GCMs over this larger zone (which encompasses the Barents, Beaufort, Chukchi, Kara, and Laptev Seas; DeWeaver 2007), so the climate predictions do apply over this larger area of inference. The demographic information is derived from just the SB (Regehr et al. 2007), but the life-history and behavior of polar bears in these regions is similar (Amstrup et al. 2007).

5.2 Coupling GCMs and demographic models

To our knowledge, there are few, if any, examples of demographic models coupled to GCMs, thus, this work represents a substantial breakthrough in the integration of two major classes of quantitative environmental analysis. There are substantial challenges to such a coupling: including (1) finding a way to link models that

[5] As we write this in August of 2007, a month prior to the end of the sea ice melt season, the decline in Arctic sea ice extent has set a new record for the available time series from1979-2006 (National Snow and Ice Data Center, http://nsidc.org/news/press/2007_seaiceminimum/20070810_index.html).

operate at substantially different spatial scales and over different time intervals, and (2) discovering a link between some environmental factor predicted by the climate models and a demographic response that can be represented in the population model. Future examples of such coupled models will require these same issues to be resolved for each new application.

Several aspects of our use of these climate models deserve comment. First, we focused on the IPCC A1B forcing scenario. This scenario projects future global CO_2 levels based on a business-as-usual assumption about future global economies and energy use. Several other forcing scenarios have been explored by IPCC, based on different assumption about patterns of CO_2 production and uptake, and these scenarios project different trends in global temperatures and other climatic variables. Thus, our results do not capture uncertainty in population projections derived from uncertainty about future patterns of atmospheric CO_2. The A1B scenario, however, enjoys support as a middle-of-the-road forecast, thus in this context, it is neither precautionary nor optimistic.

Second, we chose 10 of the global circulation models to include in our analysis, rather than the whole suite of available models. The rationale for this choice is described in a companion report (DeWeaver 2007) but was based on how well models match observed ice conditions from 1953-1995. We believe these to be the most appropriate models for forecasting arctic sea ice dynamics. Some excluded models do a very poor job of predicting sea ice, predicting either no change over the next century or complete loss of sea ice. These models would not provide useful projections.

Finally, we examined sea ice dynamics over a larger area than the southern Beaufort Sea, because of the spatial limitations of the global circulation models. To the extent that this larger area does not represent the patterns that will be seen in the SB, our projections might change if more detailed information were available. However, the use of the larger spatial area in the climate models does make us more comfortable drawing tentative inference about the population dynamics in that part of the polar basin.

5.3 Caveats

Evaluation of the strength of our conclusions requires consideration of a number of factors that went into the calculations. Below we discuss several sets of issues, examining assumptions and exploring issues that could affect our conclusions.

5.3.1 Estimation and inference

The conclusions of this report depend, in part, on the parameter estimation methods used to calculate inputs for the demographic model. Part I of this report (Regehr et al. 2007) discusses those methods in detail. However, we feel it pertinent to mention that one concern that has arisen in short-term mark-recapture studies of animals with high survival rates is the potential for negative bias in survival rates at the end of a time series, due to non-random temporary emigration. Regehr et al. (2007) carefully consider this potential source of bias, concluding that it is unlikely, but the possibility cannot be completely eliminated from any study.

Our evaluation of the effect of the frequency of bad years on population growth rate depends on using the periods 2001-2003 and 2004-2005 to characterize good and bad years, respectively. These sample sizes are small (3 and 2 years, respectively) and may not be representative of the classes of conditions we wish to encapsulate, and there is considerable uncertainty in the estimation of the growth rates for each of those years. Nevertheless, our projections take full account of this uncertainty, thus considering the possibility that the difference between the good and bad years is not as great as the means imply, or is perhaps greater. The strength of the patterns in the projections, even considering the uncertainty, is evidence of the significance of the differences among these years.

Our projections of future population trend, from the linked GCM-demographic model, are predicated on a causal relationship between sea ice extent and polar bear survival. No obser-

vational (as opposed to experimental, which is clearly impossible in this context) study can ever provide iron-clad evidence of causation. However,the fact that we only considered one explanatory variable, which was identified a priori, lends support to our argument. More importantly, our understanding of the ecology of the species clearly indicates that sea ice is an environmental factor with effects on polar bear survival and reproduction.

Finally, the models that included *ice* as a covariate were quite sensitive to uncertainty, giving rise in some cases to results that defied intuition, such as a small fraction of replicates that indicated current growth rates of 0. While this raises some concern, it is understandable as a statistical result of fitting a parametric model to a short time series. We used the non-covariate model set to explore the projections in the absence of this sensitivity. That both model sets provide the same qualitative predictions, and agree quantitatively in many instances, leads us to believe that this sensitivity does not undermine our conclusions.

5.3.2 Model structure

The conclusions of this report also depend, in part, on the structure of the demographic model. Several elements of the model structure deserve comment.

The demographic model contains no density-dependent mechanisms (either positive or negative). It is tempting to speculate that at low population sizes some compensatory mechanism might make growth rates increase because of reduced competition and provide some resilience that our model does not capture. However, a density-dependent analysis of the SB polar bear population could not be as simple as that. It would have to account for the prospect of dramatic declines in carrying capacity due to climate change. As a very crude calculation, if the carrying capacity varies with overall Arctic sea ice, it would have been declining at a rate of about 1.8% per year since 1995 (Stroeve et al. 2007). In the best of all density-dependent worlds, the population would have been tracking that decline, leading to $\lambda \approx 0.98$ without any additional effects (e.g., mortality due to drowning) of sea ice decline. To the extent that polar bears rely on sea ice on the continental shelf, near the southern edge of the Beaufort Sea, future declines would have even more dramatic impact on carrying capacity. Alternately, and perhaps more likely, if there is a depensatory mechanism (such that growth rates decrease even more because of Allee effects), then the demise of the population could be accelerated. In any event, the effects of density dependence can only be speculation, pending the development of models linking the carrying capacity and changes in the environment.

We have not included emigration or immigration in the demographic model. If there is permanent emigration from the SB population, then the estimated survival rates reflect the apparent survival rates, not the true survival rates. In this case, the population growth rate would be accurate as far as the SB population is concerned, but negatively biased relative to the contribution the SB population makes to the rangewide population (Runge et al. 2006). Likewise, if there is net immigration to the SB population from neighboring areas, which we have not included, then the current and future growth rates would not be as low as we have estimated. From the standpoint of persistence of the SB population, however, we might view emigration as equivalent to death, because the animals no longer remain in this region. Further, immigration, even if it is occurring now, is likely to become less important in the future, if the SB region does not contain suitable habitat, and if the neighboring regions begin to experience population declines. The effects of immigration and emigration could only be evaluated by developing a spatial model for polar bear populations.

We have not included demographic stochasticity in this model. Such stochasticity will accelerate extinction once the population reaches very small (10s of animals) absolute population size (Caswell 2001). If the population becomes small enough for demographic stochasticity to be important, it is already at risk simply due to

its small size. Thus this omission does not undermine any of the major conclusions. The primary results of this analysis are driven by the deterministic loss of sea ice and the concomitant reduction in survival; stochastic effects add variance to this pattern, but do not change the general trends.

Finally, of course, no model constructed in the present can predict how polar bears might respond behaviorally to substantial changes in their environment in the future. As summer ice in the SB region retreats beyond the continental shelf, one might speculate that polar bears could develop a new strategy for seeking food (e.g., by becoming more land-based), they could emigrate out of the region, or they could continue to remain in the area. Our projections can only assume that they remain in the area (and face reduced survival) or emigrate out of the area (and be effectively dead as far as the SB management unit is concerned). But, as polar bears are one of the most mobile of quadrupeds, and have evolved in a highly dynamic environment, one might speculate they could adapt in some manner. However, all studies to date of annual movement patterns of polar bears indicate a very high degree of fidelity to their natal populations, including in SB and western Hudson Bay, where they are already being significantly and negatively affected by changes in ice conditions. Further, the potential nutritive benefits of terrestrial feeding are calorically insignificant and unlikely to provide a panacea.

5.4 Importance of this work

This work was motivated by the need for a status assessment to inform a regulatory decision. It was facilitated by the existence of intensive on-going field work in, and a long-term study of, the SB polar bear population, and an intensive although short-term capture-recapture study from 2001–2006.

Our work provides decision-makers with the scientific information needed to evaluate the significance of the threat of the decline in the extent of sea ice to the SB polar bear population. The results quantify the risk of decline over the next 4 to 10 decades based on current knowledge, and taking into account uncertainty that arises from parameter estimation, a short time-series of capture-recapture data, the form of the population model, environmental variation, and climate projections. The results are probabilistic, in order to represent the uncertainty that arises from all of these sources. Decision-makers will need to grapple with how that uncertainty affects the conclusion they make. In a risk analytic framework, decision-makers could use this information by identifying the event of concern, deciding what level of risk (what probability) would trigger a particular decision, and interpreting this analysis to see if that level of risk was reached.

5.5 Prospects for further demographic modeling

One of the advantages of matrix population models is that their construction lays bare the processes which are included, and those which are excluded, from any particular model. We note here that further demographic modeling would lead to further understanding of the dynamics of this population. Spatial models (using the multiregional matrix model formulation of Hunter and Caswell 2005b) and subsidized models (e.g., Caswell 2007) could consider immigration and emigration. An extension of the capture-recapture study in the SB would eventually permit quantitative rather than qualitative ("good" vs. "bad") links to climate (an example of one way to approach this is Lawler et al. 2007). A connection to resource and habitat models could help to develop a density-dependent analysis.

The polar bear is a top predator in a rapidly changing ecosystem. Further analysis of polar bear populations will not only be important for management of the species, but will play a critical role in understanding the entire Arctic ecosystem.

6 Summary and Conclusions

Demographic analysis links the condition of the environment to the fates of individuals and the fates of individuals to the dynamics of populations. Reflecting these linkages, we can describe our results in terms of a particular set of goals:

Goal 1. To evaluate the status of the southern Beaufort Sea polar bear population in terms of its current potential for population growth in both deterministic and stochastic environments.

1. If conditions over the period 2001–2005 remained constant they would lead to a nearly stationary population with a decline of about 0.3% per year.
2. The population would be capable of increasing if conditions experienced in 2001–2003 were maintained. The population would decline dramatically if conditions in 2004–2005 persisted.
3. A frequency of years with conditions similar to 2004–2005 ("bad" years) greater than a critical value of about 0.17 would lead to population decline. The observed frequency of bad years since 1979 is approximately 0.21, and appears to have been increasing.
4. A stochastic environment in which good (2001–2003) and bad (2004–2005) years occurred at the frequency observed since 1979 would lead to population decline at a rate of about 1% per year.
5. Population growth rate (both deterministic and stochastic) is most elastic to adult female survival and, to a lesser degree, breeding probability.

Goal 2. To quantify the response of population growth to the number of ice free days over the continental shelf.

1. The deterministic population growth rate showed a marked decrease above a threshold number of ice-free days (≈ 125) over the continental shelf. A similar decrease in population growth rate in the last two years, which had above normal ice-free periods, was observed from non-covariate models.
2. The stochastic growth rate declines with increasing frequency of occurrence of years with above normal ice-free days. An increase of 0.1 in the frequency of such years reduces the population growth rate by 2–3 percentage points per year.

Goal 3. To project future population growth on a time scale of decades to a century, in constant environments, in stochastic environments, and in environments forecast by global climate models.

1. If conditions were to remain similar to 2001-2003, the population would increase over the next 45-100 years. If conditions remained similar to 2004-2005, the population would decline precipitously within 45 years.
2. In a stochastic environment with a frequency of bad years equal to the observed value over the period 1979-2006, the population would probably decline to between 1% and 10% of its current size before the end of the century.
3. A stochastic environment described by forecasts of sea ice conditions from a suite of 10 GCMs all lead to crashes of the population within the next 100 years, usually within the next 50 years.
4. The current population structure is close to the stable stage distribution, so asymptotic population growth rates provide accurate descriptions of relatively short-term (45 year) projections.

Goal 4. To evaluate the effects of uncertainty in parameter estimates and model selec-

tion on population growth rate and population projections.

1. Parametric bootstrap approaches permit us to document the probability of outcomes based on the sampling uncertainty. In no case does the uncertainty change the conclusions of the analysis.

The intent of this analysis was to integrate climate projections indicative of polar bear habitat with demographic models of polar bear population dynamics and to evaluate the severity of the threat faced by polar bears in the southern Beaufort Sea due to changes in sea ice. We focused on the increasing number of ice-free days over water 300m in depth or less. This represents the areas where ringed seals in the SB are most abundant (Stirling et al. 1982). Our analysis suggests that polar bears in the SB are likely to experience an important decline by mid-century as the Arctic ocean becomes increasingly ice free in the summer.

7 Acknowledgments

C. Hunter and H. Caswell acknowledge funding for model development and analysis from the U.S. Geological Survey and U.S. Fish and Wildlife Service, the National Science Foundation, NOAA, the Ocean Life Institute at WHOI, and the Institute of Arctic Biology at the University of Alaska Fairbanks. Funding for the capture-recapture effort in 2001-2006 was provided by the U.S. Geological Survey, the Canadian Wildlife Service, the Department of Environment and Natural Resources of the Government of the Northwest Territories, and the Polar Continental Shelf Project, Ottawa, Canada. We thank G.S. York, K.S. Simac, M. Lockhart, C. Kirk, K. Knott, E. Richardson, A.E. Derocher, and D. Andriashek for assistance in the field. D. Douglas and G. Durner assisted with analyses of radiotelemetry and remote sensing sea ice data. J. Nichols, and M. Udevitz provided advice with data analysis. We thank E. Cooch, J-D. Lebreton, and J. Nichols for helpful comments and discussions. Funding for this analysis was provided by the U.S. Geological Survey and U.S. Fish and Wildlife Service.

8 Literature cited

Aars, J., N.J. Lunn, and A.E. Derocher. 2006. Polar Bears: Proceedings of the 14th Working Meeting of the IUCN/SSC Polar Bear Specialists Group. International Union for Conservation of Nature and Natural Resources, Gland, Switzerland and Cambridge, United Kingdom.

Amstrup, S.C. 2003. Polar bear, *Ursus maritimus*. pp. 587–610 in G.A. Feldhamer, B.C. Thompson, and J.A. Chapman, editors. Mammals of North America: biology, management, and conservation. Johns Hopkins University Press, Baltimore, Maryland, USA.

Amstrup, S.C., and C. Gardner. 1994. Polar bear maternity denning in the Beaufort Sea. Journal of Wildlife Management 58:1-10.

Amstrup, S.C., B.G. Marcot, and D.C. Douglas. 2007. Forecasting the rangewide status of polar bears at selected times in the 21st century. USGS Alaska Science Center, Anchorage, Administrative Report.

Amstrup, S.C., T.L. McDonald, and I. Stirling. 2001. Polar bears in the Beaufort Sea: A 30 year mark-recapture case history. Journal of Agricultural, Biological, and Environmental Statistics 6:221–234.

Amstrup, S.C., I. Stirling, and J.W. Lentfer. 1986. Past and present status of polar bears in Alaska. Wildlife Society Bulletin 14:241–254.

Brower, C.D., A. Carpenter, M.L. Branigan, W. Calvert, T. Evans, A.S. Fischbach, J.A. Nagy, S. Schliebe, and I. Stirling. 2002. The polar bear management agreement for the southern Beaufort Sea: An evaluation of the first ten years of a unique conservation agreement. Arctic 55:362–372.

Burnham, K. P., and D. R. Anderson. 2002.

Model Selection and Multimodel Inference: A Practical Information-Theoretic Approach. Second edition. Springer-Verlag, New York, New York, USA. 488 pp.

Caswell, H. 1978. A general formula for the sensitivity of population growth rate to changes in life history parameters. Theoretical Population Biology 14:215–230.

Caswell, H. 1989. The analysis of life table response experiments. I. Decomposition of effects on population growth rate. Ecological Modelling 46:221–237.

Caswell H. 2001. Matrix population models. Second edition. Sinauer, Sunderland, Massachusetts, USA

Caswell H. 2005. Sensitivity analysis of the stochastic growth rate: Three extensions. Australian and New Zealand Journal of Statistics 47:75–85.

Caswell H. 2007. Sensitivity analysis of transient population dynamics. Ecology Letters 10:1–15.

Caswell H, Fujiwara M (2004) Beyond survival estimation: markrecapture, matrix population models, and population dynamics. Animal Biodiversity and Conservation 27:471–488.

Caswell, H., and T. Kaye. 2001. Stochastic demography and conservation of an endangered plant (*Lomatium bradshawii*) in a dynamic fire regime. Advances in Ecological Research 32:1–51.

Comiso, J.C. 2006. Arctic warming signals from satellite observations. Weather. 61(3):70–76.

Copas, J.B. 1983. Plotting p against x. Applied Statistics 32:25–31.

Derocher, A.E., and I. Stirling. 1992. The population dynamics of polar bears in western Hudson Bay. Pages 1150–1159 in D. R. McCullough and R. H. Barrett, editors. Wildlife 2001: Populations. Elsevier Applied Science.

DeWeaver, E. 2007. Uncertainty in climate model projections of Arctic sea ice decline: An evaluation relevant to polar bears. USGS Alaska Science Center, Anchorage, Administrative Report.

Durner, G.M., S.C. Amstrup, R.M. Nielson, and T.L. McDonald. 2004. The use of sea ice habitat by female polar bears in the Beaufort Sea. Minerals Management Service OCS Study 2004–14.

Durner, G.M., D.C. Douglas, R.M. Nielson, S.C. Amstrup, and T.L. McDonald. 2007. Predicting the future distribution of polar bear habitat in the Polar Basin from resource selection functions applied to 21st cdentury general circulation model projections of sea ice. USGS Alaska Science Center, Anchorage, Administrative Report.

Efron, B., and R.J. Tibshirani. 1993. An Introduction to the Bootstrap. Chapman and Hall.

Fujiwara, M. and H. Caswell. 2001. Demography of the endangered North Atlantic right whale. Nature 414:537-541.

Fujiwara M, and H. Caswell. 2002. Estimating population projection matrices from multistage mark-recapture data. Ecology 83:3257–3265.

Gaston, A.J., H.G. Gilchrist, and J.M. Hipfner. 2005. Climate change, ice conditions, and reproduction in an Arctic nesting marine bird: Brunnich's guillemot (Uria lomvia L.). Journal of Animal Ecology 74:832–841.

Gervais, J. A., C. M. Hunter, and R. G. Anthony. 2006. Interactive effects of prey and p,p' DDE on burrowing owl population dynamics. Ecological Applications 16:666-677.

Heppell, S.S., H. Caswell, and L.B. Crowder. 2000. Life histories and elasticity patterns: Perturbation analysis for species with minimal demographic data. Ecology 81:654–665.

Hunter, C.M. and H. Caswell. 2005a. Selective harvest of sooty shearwater chicks: effects on population dynamics and sensitivity. Journal of Animal Ecology 74:589-600.

Hunter, C.M. and H. Caswell. 2005b. The use of the vec-permutation matrix in spatial matrix population models. Ecological Modelling 188:15-21.

IPCC, 2007: Summary for Policymakers. In: Climate Change 2007: The Physical Sci-

ence Basis. Contribution of Working Group I to the Fourth Assessment Report of the Intergovernmental Panel on Climate Change [Solomon, S., D. Qin, M. Manning, Z. Chen, M. Marquis, K.B. Averyt, M.Tignor and H.L. Miller (eds.)]. Cambridge University Press, New York, NY, USA

Lawler, R.L., H. Caswell, A.F. Richard, J. Ratsirarson, R.E. Dewar, and M. Schwartz. 2007. Demographic analysis of a protected lemur population in southwest Madagascar. Submitted.

Overland, J.E. and M. Wang. 2007. Future regional Arctic sea ice declines. Geophysical Research Letters 34: In press.

Regehr, E. V., S. C. Amstrup, and I. Stirling. 2006. Polar bear population status in the southern Beaufort Sea. U.S. Geological Survey Open-File Report 2006-1337.

Regehr, E.V., C.M. Hunter, H. Caswell, I. Stirling, and S.C. Amstrup . 2007. Polar bears in the southern Beaufort Sea I: survival and breeding in relation to sea ice conditions, 2001–2006. USGS Alaska Science Center, Anchorage, Administrative Report.

Richter-Menge, J., J. Overland, A. Proshutinsky, V. Romanovsky, L. Bengtsson, L. Brigham, M. Dyurgerov, J.C. Gascard, S. Gerland, R. Graversen, C. Haas, M. Karcher, P. Kuhry, J. Maslanik, H. Melling, W. Maslowski, J. Morison, D. Perovich, R. Przybylak, V. Rachold, I. Rigor, A. Shiklomanov, J. Stroeve, D. Walker, and J. Walsh. 2006. State of the Arctic Report. NOAA OAR Special Report, NOAA/OAR/PMEL, Seattle, WA, 36 pp.

Rigor, I.G., and J.M. Wallace. 2004. Variations in the age of Arctic sea-ice and summer sea-ice extent. Geophysical Research Letters. 31:L09401.

Runge, J.P., M.C. Runge, and J.D. Nichols. 2006. The role of local populations within a landscape context: defining and classifying sources and sinks. American Naturalist 167:925–938.

Runge, M. C., C. A. Langtimm and W. L. Kendall. 2004. A stage-based model of manatee population dynamics. Marine Mammal Science 20:361-385.

Smith M, H. Caswell and P. Mettler-Cherry 2005. Stochastic flood and precipitation regimes and the population dynamics of a threatened floodplain plant. Ecological Applications 15:1036–1052.

Stirling, I. 1988. Polar bears. University of Michigan Press, Ann Arbor, Michigan, USA.

Stirling, I., M. Kingsley, and Calvert, W. 1982. The distribution and abundance of seals in the eastern Beaufort Sea, 1974-79. Canadian Wildlife Service Occasional Paper 47. 23 pp.

Stirling, I., T.L. McDonald, E.S. Richardson, and E.V. Regehr. 2007. Polar bear population status in the northern Beaufort Sea. USGS Alaska Science Center, Anchorage, Administrative Report.

Stroeve, J.C., M.M. Holland, W. Meier, T. Scambos, and M. Serreze. 2007. Arctic sea ice decline: Faster than forecast. Geophysical Research Letters 34(9):L09501, doi:10.1029 /2007GL029703.

Tuljapurkar, S. 1990. Population dynamics in variable environments. Springer-Verlag, New York, New York, USA.

U.S. Fish and Wildlife Service. 2007. Endangered and threatened wildlife and plants: 12-month petition finding and proposed rule to list the polar bear (*Ursus maritimus*) as threatened throughout its range. Federal Register 72(5):1064–1099.

9 Tables

Table 1: Deterministic population growth rate λ, with 90% confidence intervals, standard error, and proportion of bootstrap samples < 1, for the time-invariant, full, and non-covariate model sets.

Model set	Year	λ	lower CI	upper CI	SE	proportion < 1
time-invariant		0.997	0.755	1.053	0.105	0.57
full	2001	1.059	0.083	1.093	0.269	0.24
	2002	1.061	0.109	1.094	0.265	0.24
	2003	1.036	0.476	1.107	0.207	0.41
	2004	0.765	0.541	0.932	0.120	1.00
	2005	0.799	0.577	0.959	0.122	0.99
non-cov	2001	1.017	0.810	1.088	0.092	0.43
	2002	1.022	0.836	1.088	0.084	0.40
	2003	1.075	0.903	1.129	0.077	0.19
	2004	0.801	0.549	1.000	0.135	0.95
	2005	0.895	0.446	1.020	0.185	0.88

Table 2: Ten IPCC AR-4 GCMs used to forecast ice covariates. IPCC model name, country of origin, approximate grid resolution (degrees), and the number of runs used for demographic projections.

IPCC model name	Country	Grid resolution	Runs
ncar_ccsm3_0	USA	1.0×1.0	8
cccma_cgcm3_1	Canada	3.8×3.8	1
cnrm_cm3	France	1.0×2.0	1
gfdl_cm2_0	USA	0.9×1.0	1
giss_aom	USA	3.0×4.0	1
ukmo_hadgem1	UK	0.8×1.0	1
ipsl_cm4	France	1.0×2.0	1
miroc3_2_medres	Japan	1.0×1.4	1
miub_echo_g	Germany/Korea	1.5×2.8	1
mpi_echam5	Germany	1.0×1.0	1

10 Figures

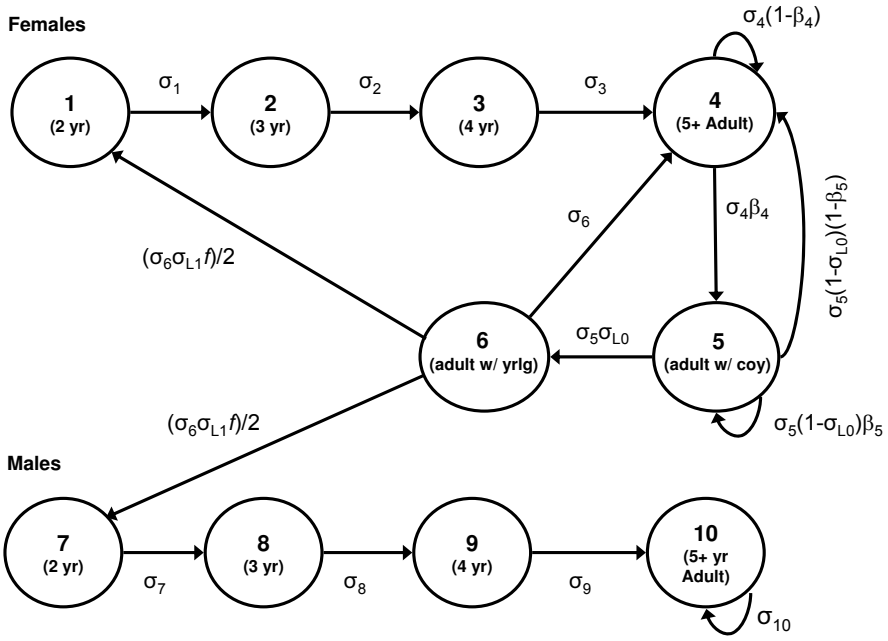

Figure 1: The polar bear life cycle graph; stages 1–6 are females and stages 7–10 are males. σ_i is the probability of survival of an individual in stage i, σ_{L0} and σ_{L1} are the probability of at least one member of a cub-of-the-year (COY) or yearling litter surviving to the following spring, f is the expected size of yearling litters that survive to 2 years, and β_i is the conditional probability, given survival, of an individual in stage i breeding, thereby producing a COY litter with at least one member surviving until the following spring.

10.1 Deterministic model figures

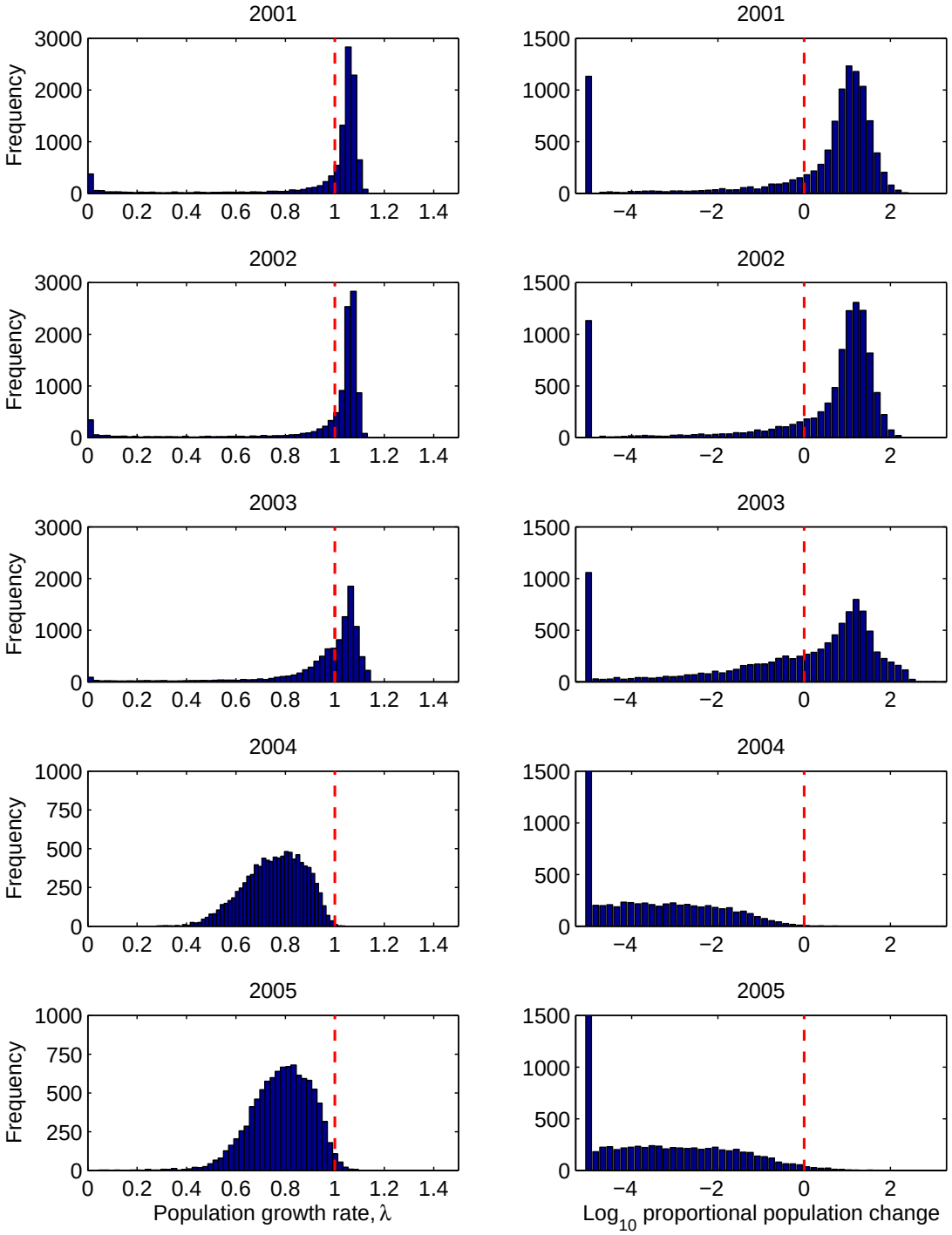

Figure 2: Bootstrap distribution of deterministic population growth rates (left column) and log of population size at 45 years relative to starting population size (right column), from the full model set for conditions in 2001–2005. Bar at left of histogram (right column) gives all instances below axis minimum. Bootstrap sample size $B = 10,000$.

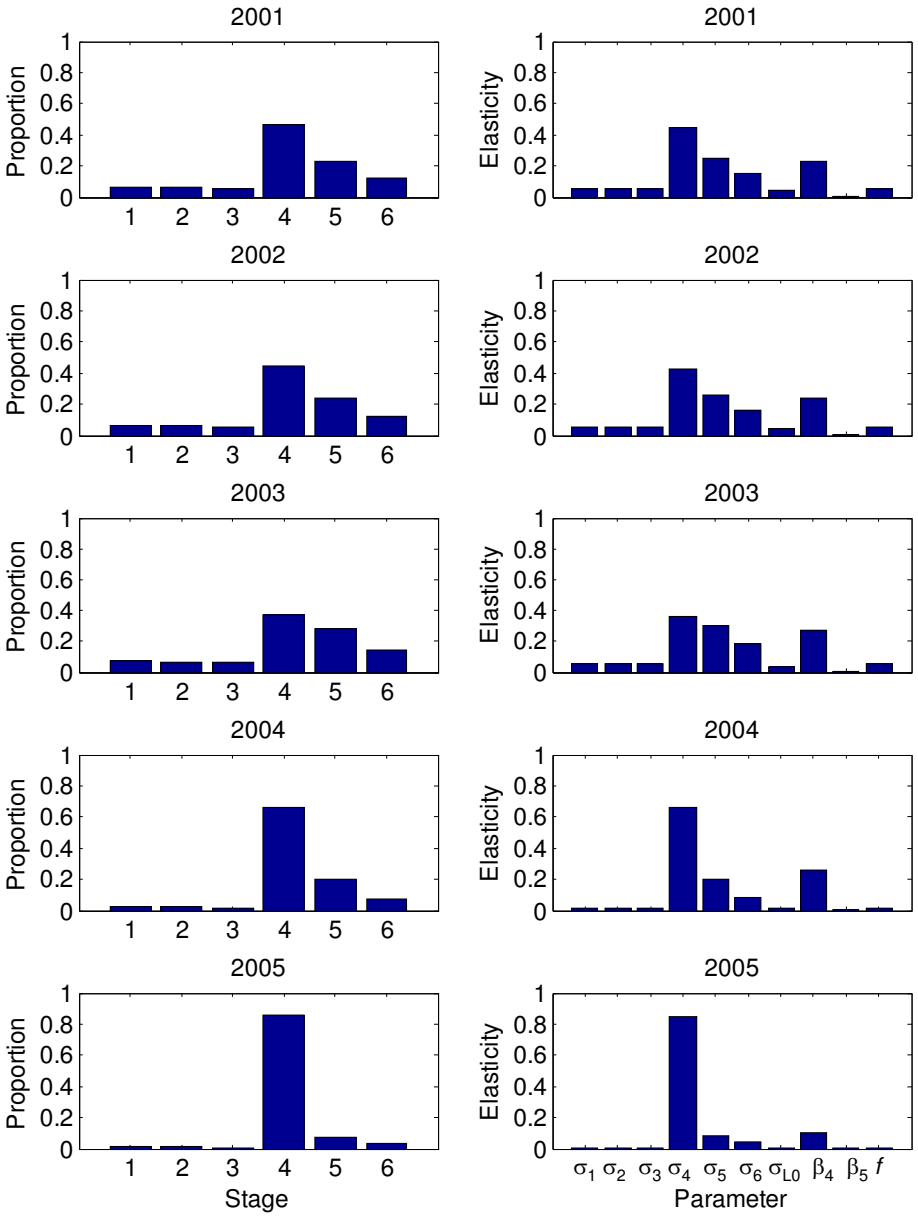

Figure 3: Stable stage distribution (left column) and elasticity of λ to model-averaged parameter estimates (right column) from the full model set for conditions in 2001–2005.

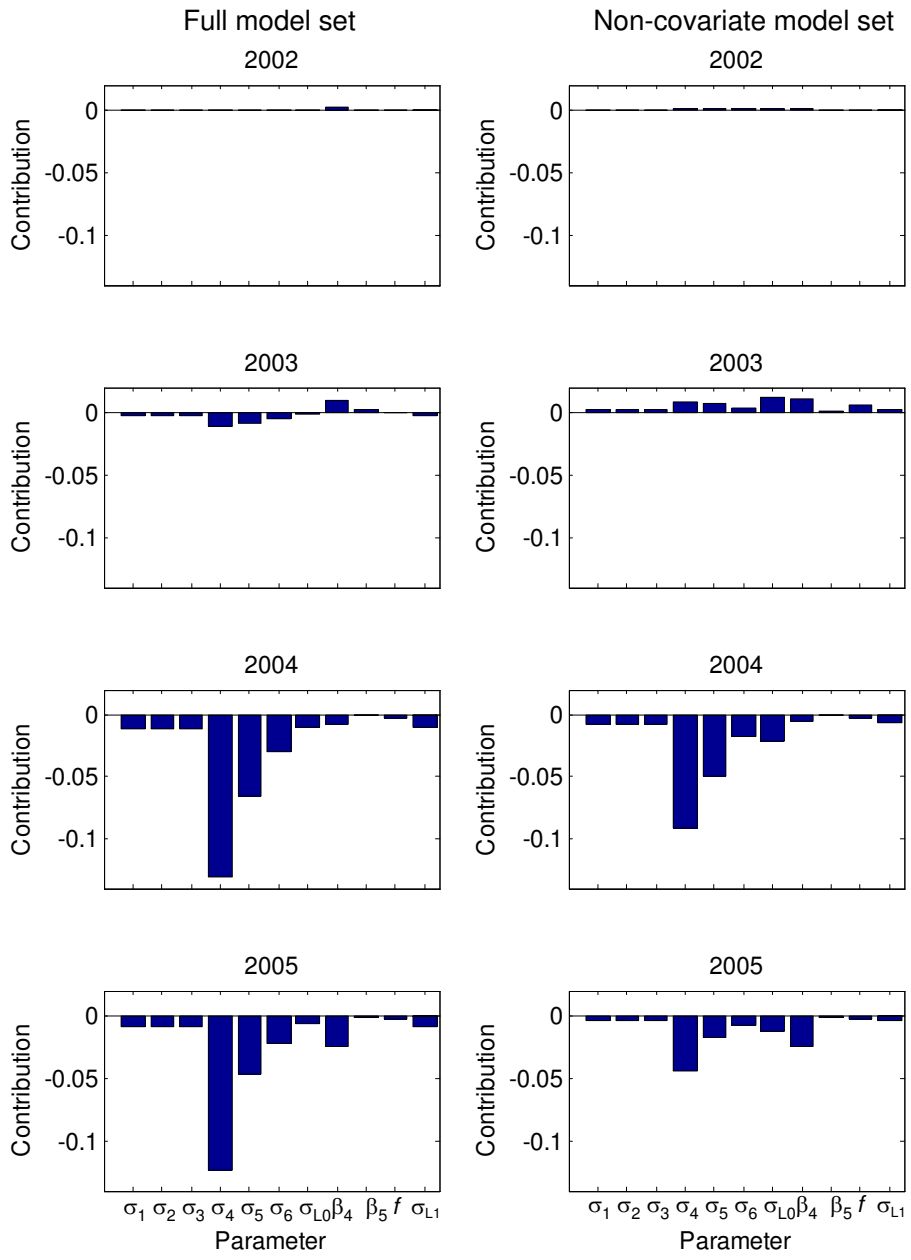

Figure 4: LTRE decomposition of the contributions to differences in λ of parameters from the full model (left column) and the non-covariate model set for 2002–2005. Differences are measured relative to conditions in 2001.

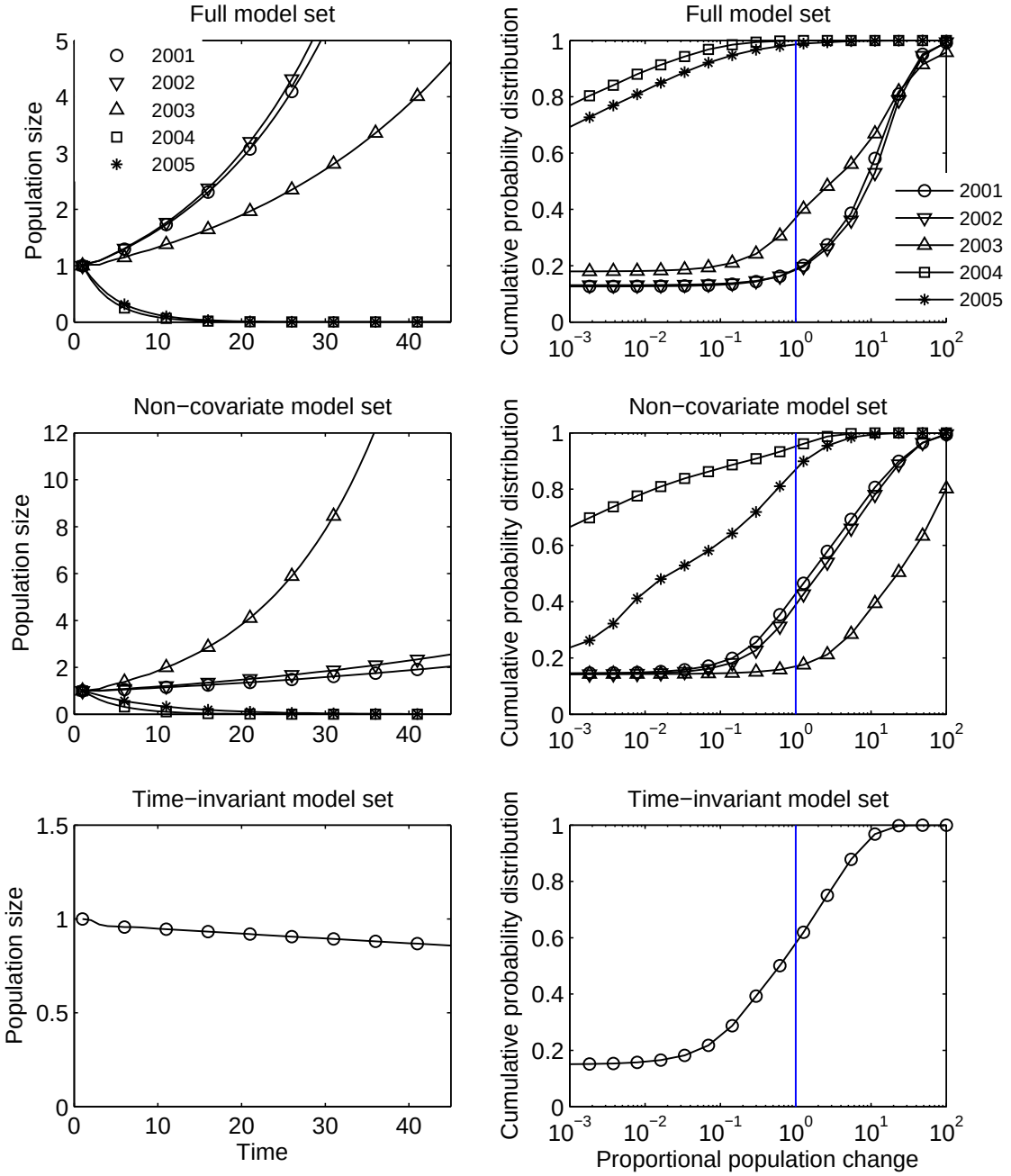

Figure 5: 45-year population projections (left column) for parameter estimates from the full, non-covariate and time-invariant model sets. Cumulative bootstrap probability distribution (right column) of the log of population size at 45 years relative to the starting population size, from the full, non-covariate and time-invariant model sets.

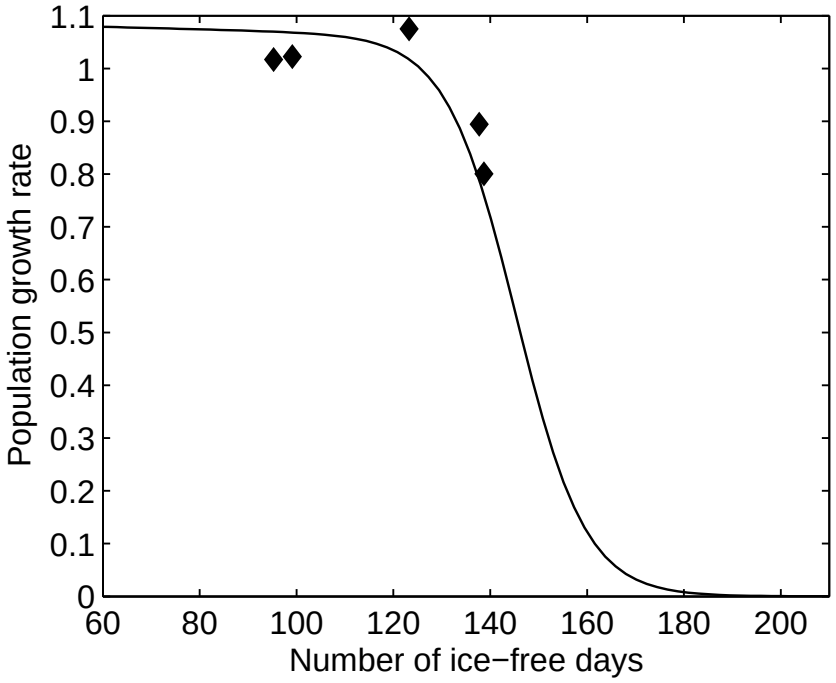

Figure 6: Solid line: population growth rate λ as a function of the ice covariate estimated from the full model set. Diamonds: population growth rate estimated for 2001–2005 from the non-covariate model set.

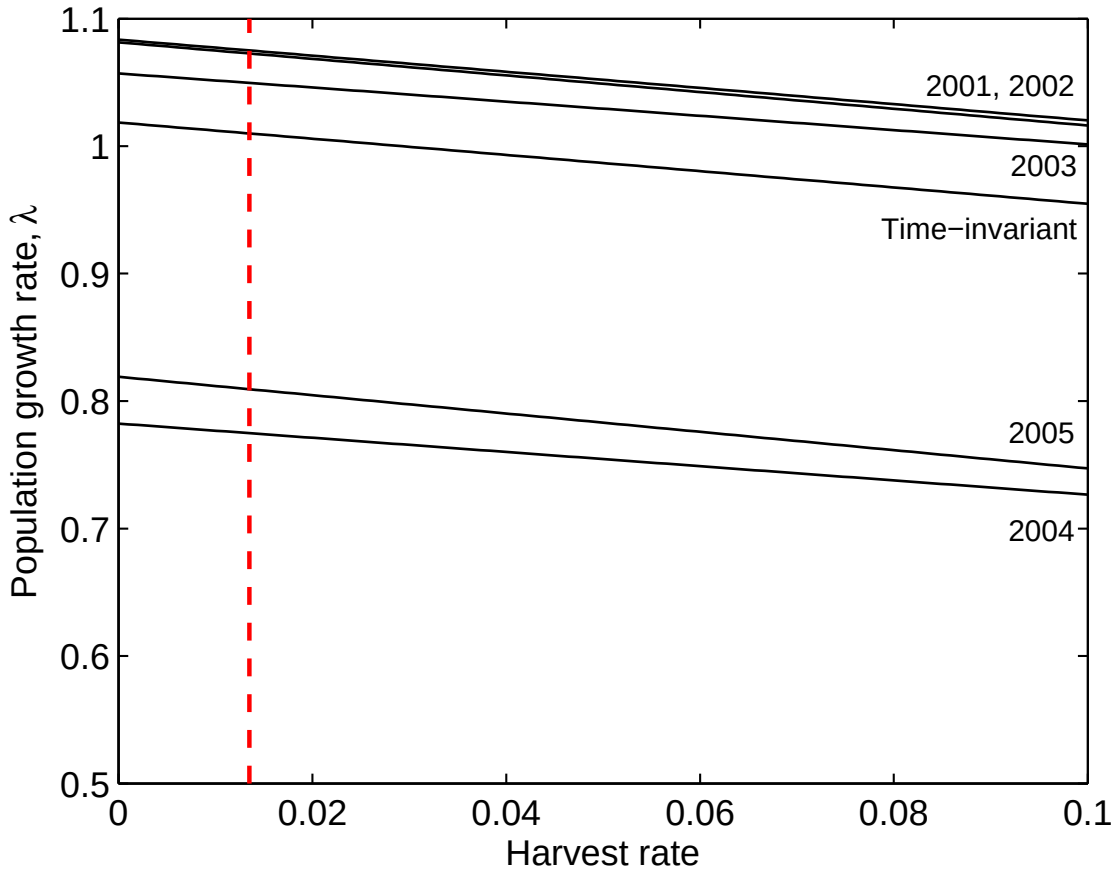

Figure 7: Population growth rate, λ, as a function of harvest rate for model-averaged parameter estimates from the full model set for 2001–2005 and for time-invariant estimates. Harvest is assumed to affect only stages 1–4. The vertical dashed line is the estimated harvest rate of females without dependent young.

10.2 Stochastic model figures

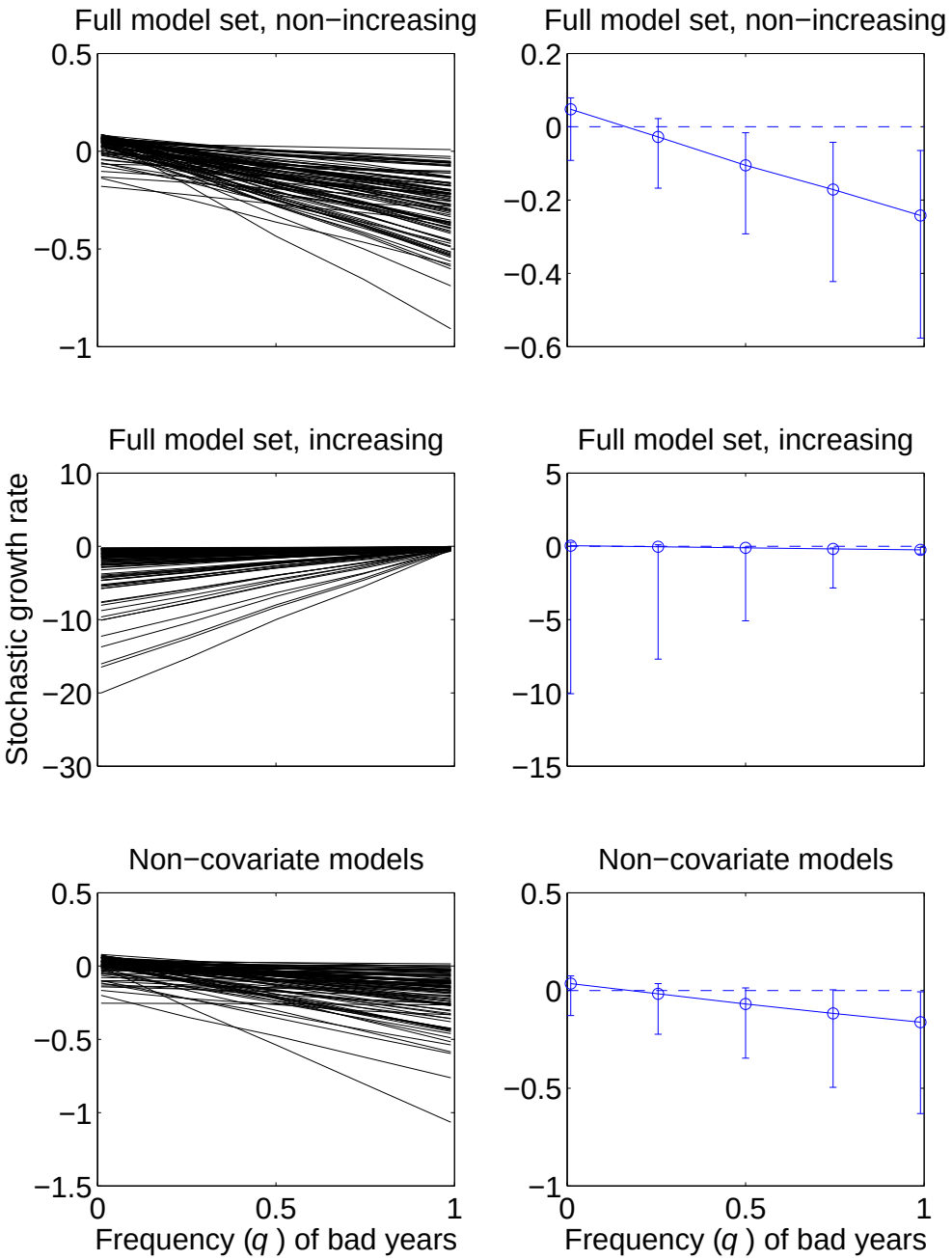

Figure 8: The stochastic growth rate $\log \lambda_s$ as a function of the frequency q of years with greater than 127 ice-free days. Multiple lines show a sample of 100 models from the bootstrap distribution of (from top to bottom) the full model set conditional on non-increasing response, the full model set conditional on increasing response, and the non-covariate model set. The right panels show the estimates of $\log \lambda_s$ and 90% parametric bootstrap confidence intervals.

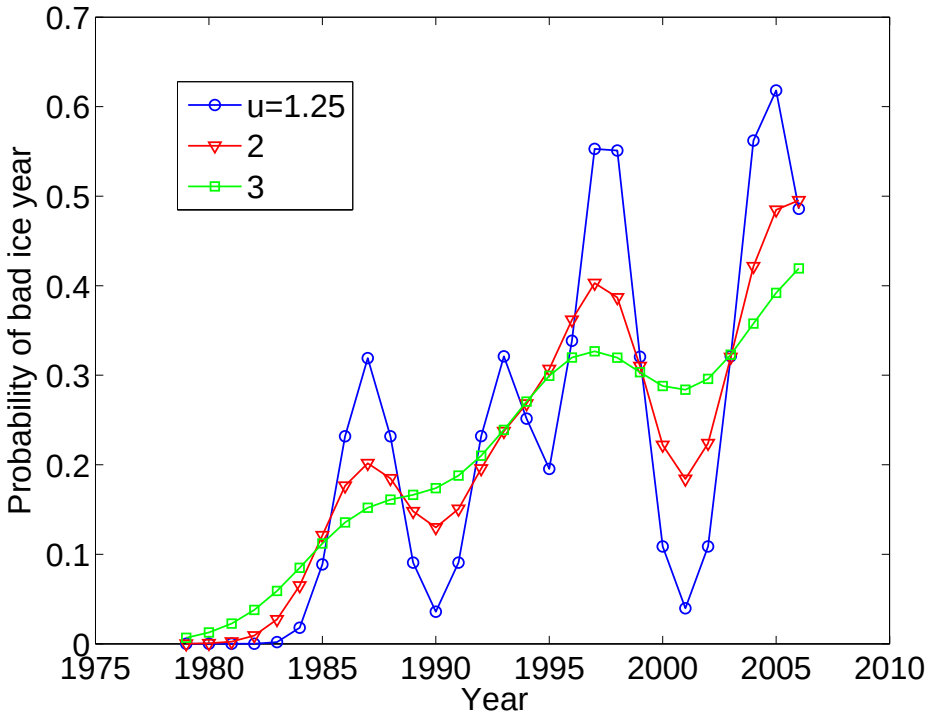

Figure 9: Frequency of bad ice conditions from 1979–2006, smoothed with a Gaussian kernel smoother with standard deviation $u = 1.5, 2, 3$ (Copas 1983). Data from Figure 3 in Part I of this report (Regehr et al. 2007).

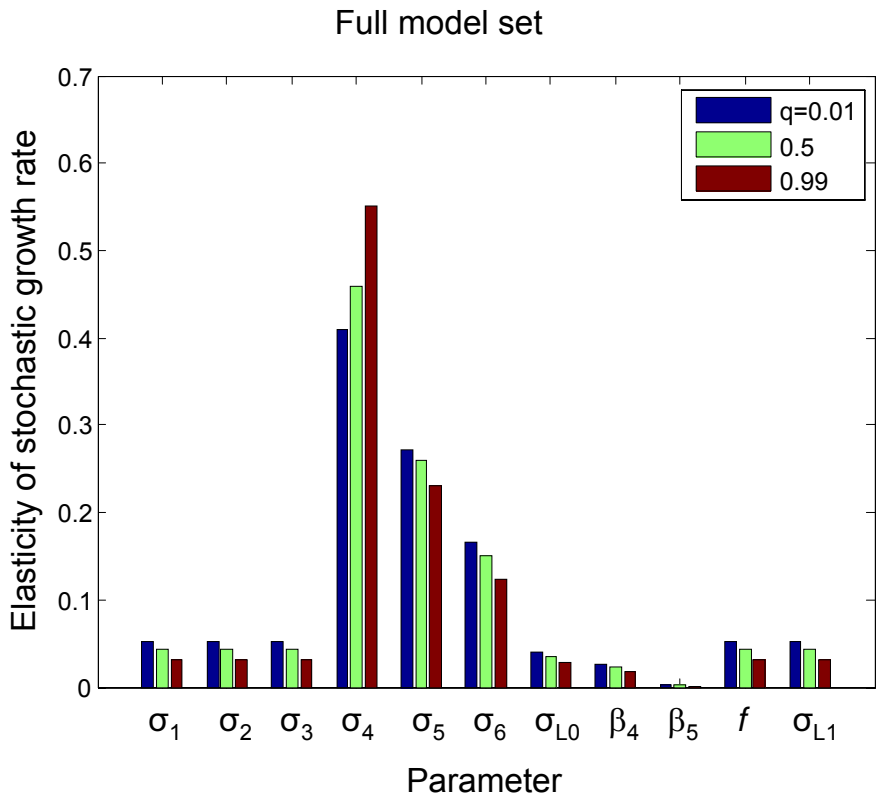

Figure 10: Elasticity of the stochastic growth rate λ_s for three values of the probability q of bad ice conditions for parameter estimates from the full model set.

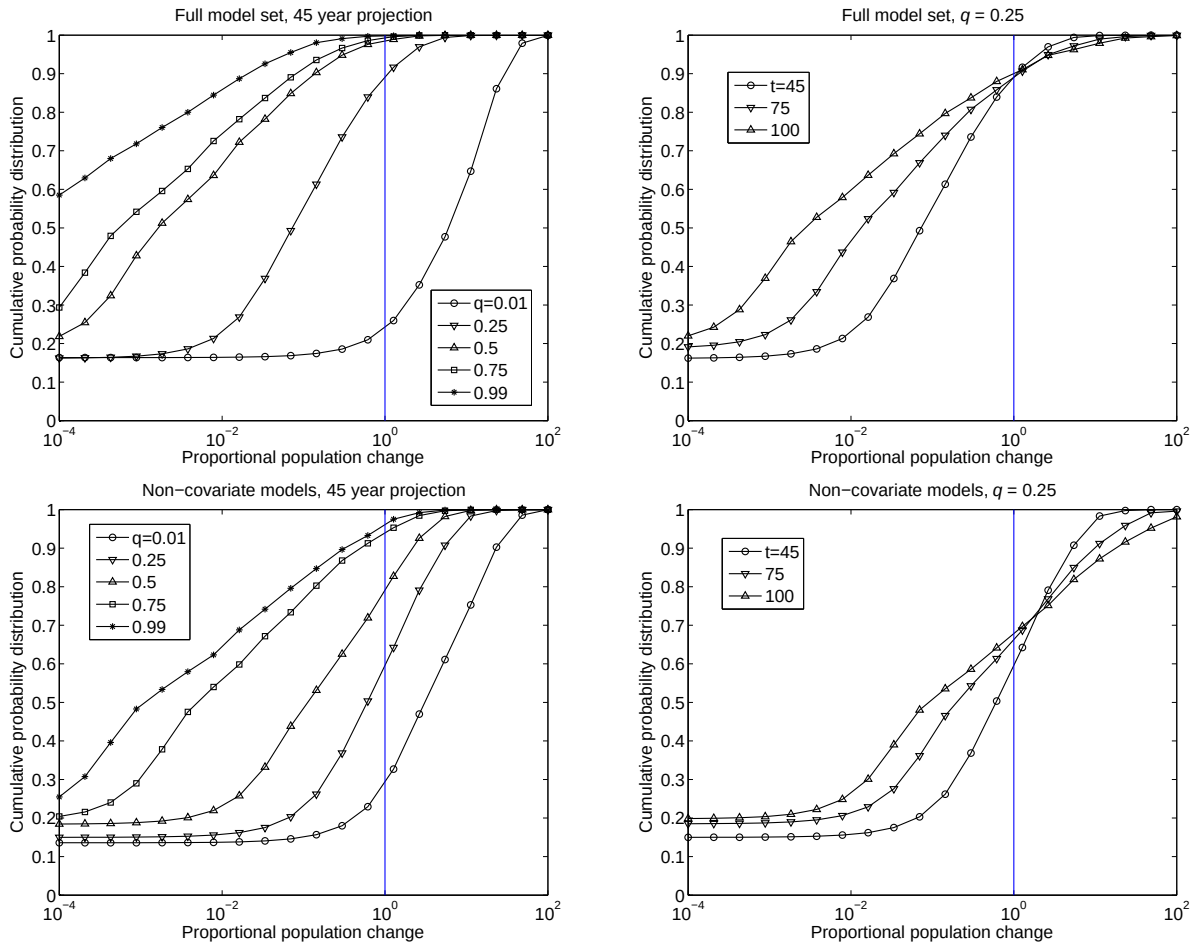

Figure 11: Cumulative distribution of population change from the full and non-covariate model sets. Left panels show the cdf at $t = 45$ years as a function of the frequency q of bad years. Right panels show the cdf at 45, 75, and 100 years for $q = 0.25$. Bootstrap sample of size $B = 2000$.

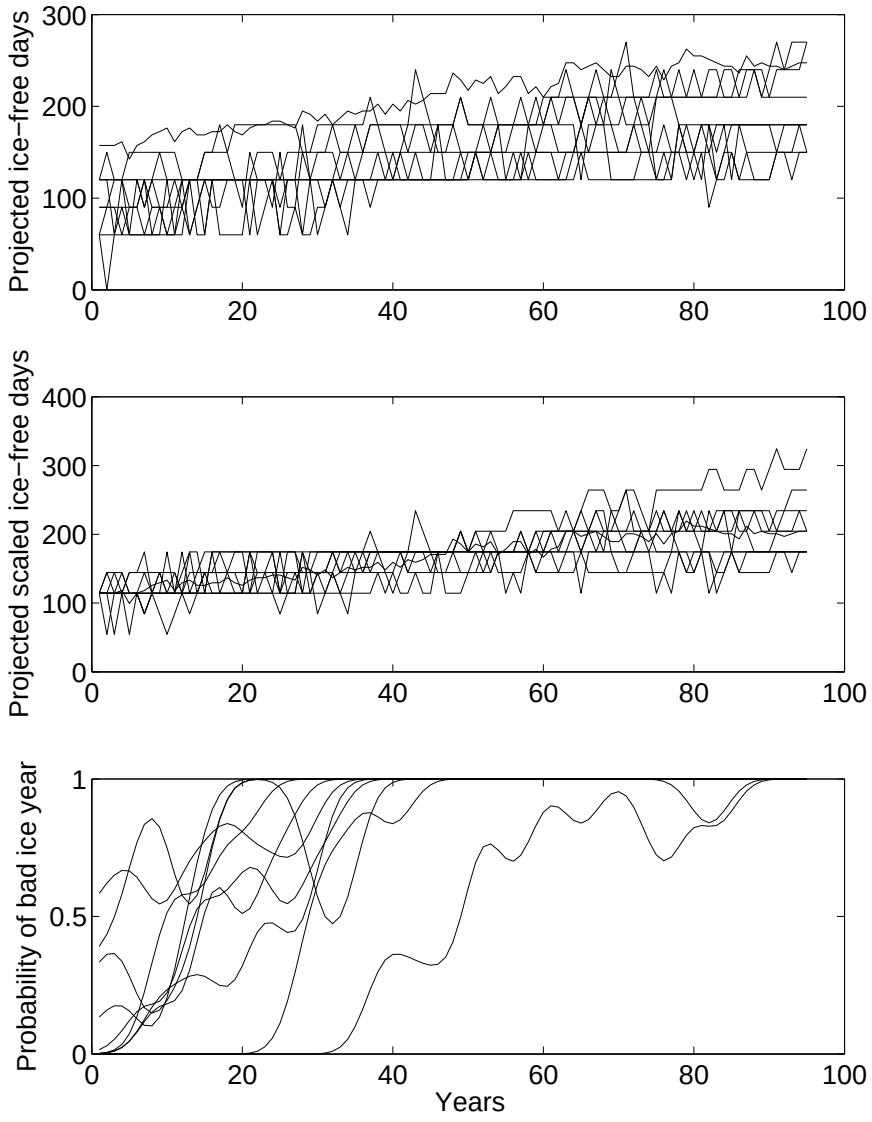

Figure 12: Upper panel: projected ice-free days from each of 10 climate models, from 2005–2100. Middle panel: projected ice free days rescaled to agree with the observed average ice-free days from 2000–2005. Lower panel: the projected probability of a bad ice year, from 2005–2100, from all 10 climate models.

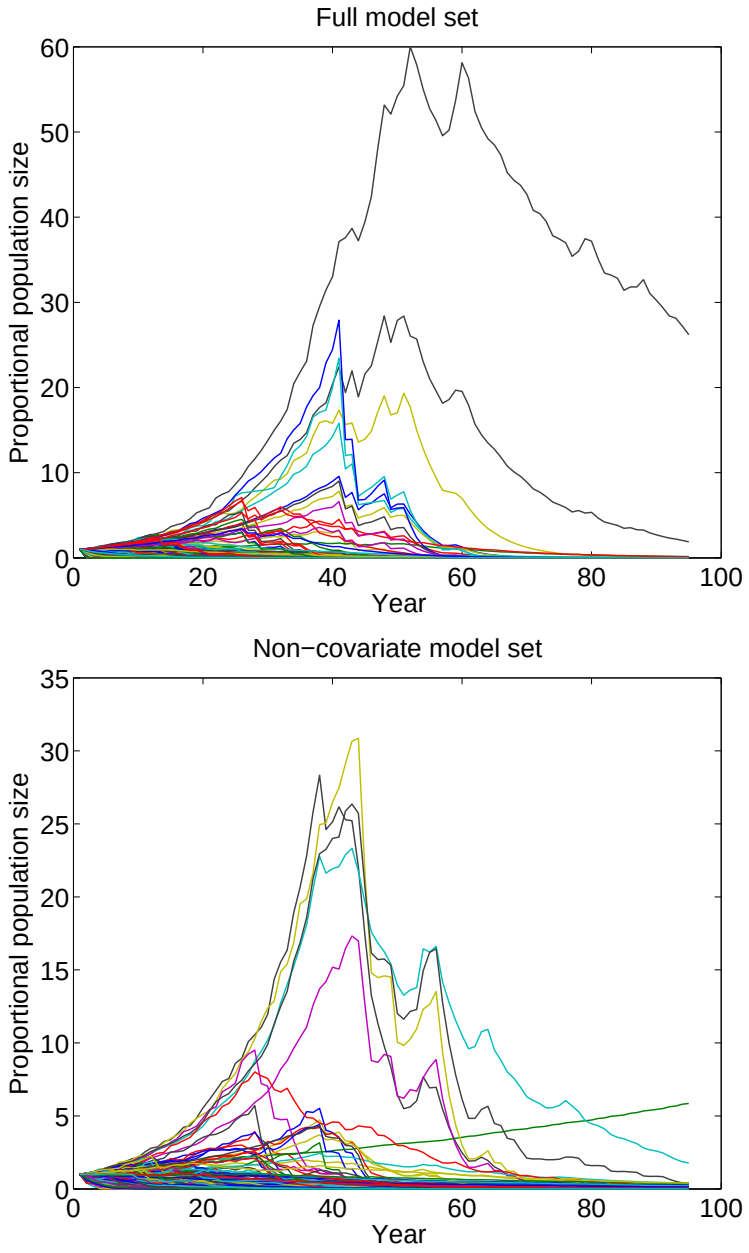

Figure 13: Stochastic projections based on climate models. Plotted are 200 bootstrap samples taken over both vital rate variability and all 10 climate models.

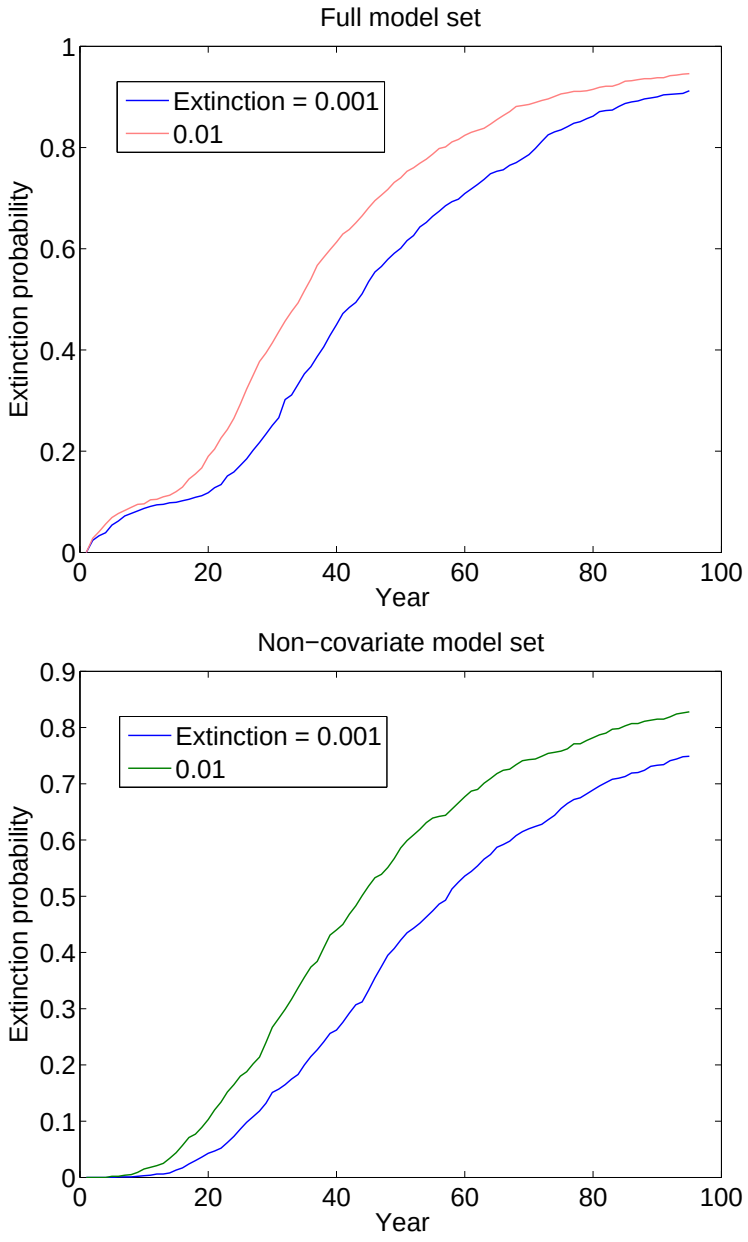

Figure 14: Probability of quasi-extinction, defined as a decline to a fraction 0.001 or 0.01 of initial population size, obtained from 1000 bootstrap samples combining all 10 climate models.

A Appendix figures

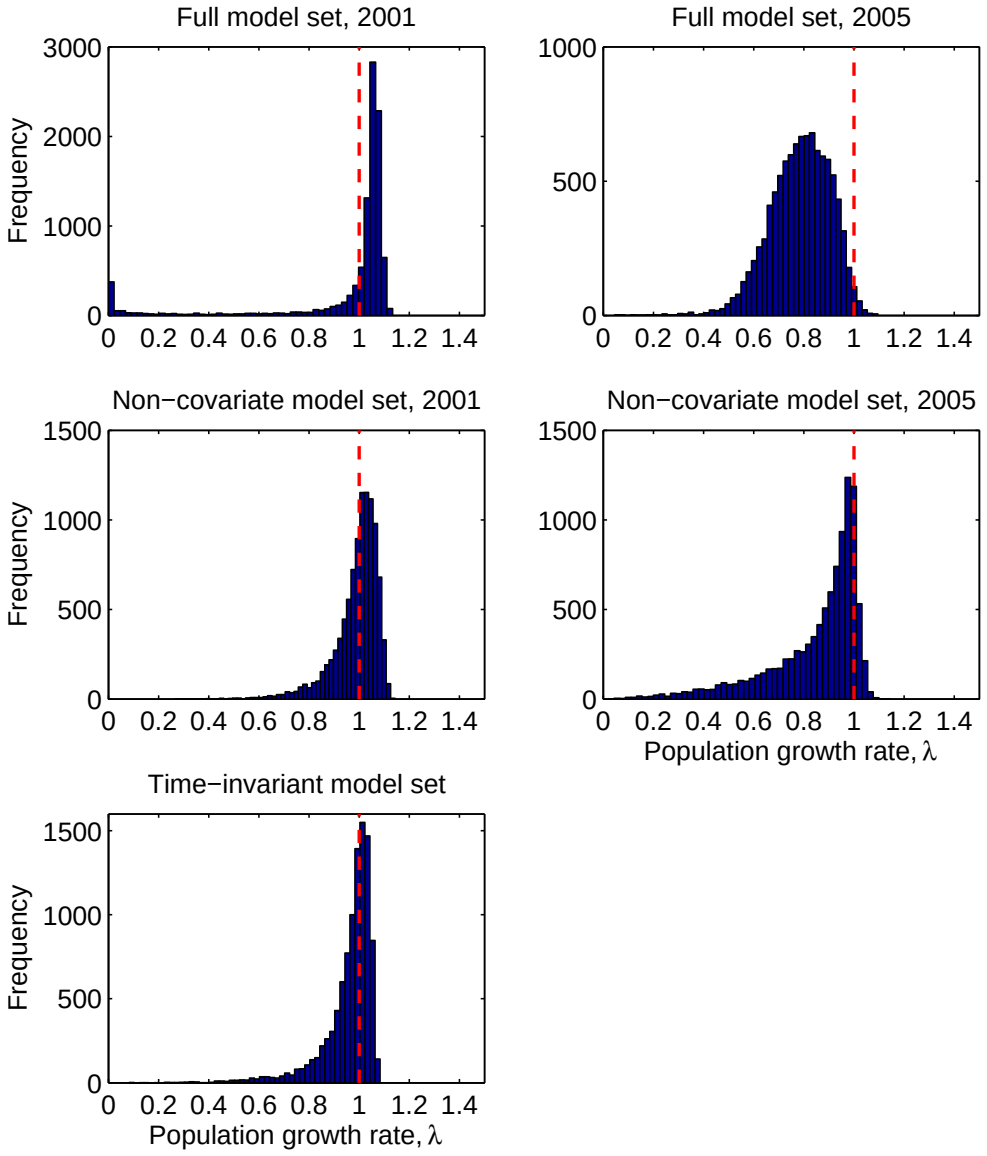

Figure A-1: Bootstrap distributions of deterministic population growth rates, λ, from the full, non-covariate and time-invariant model sets for conditions in 2001 and 2005. Bootstrap sample size $B = 10,000$.

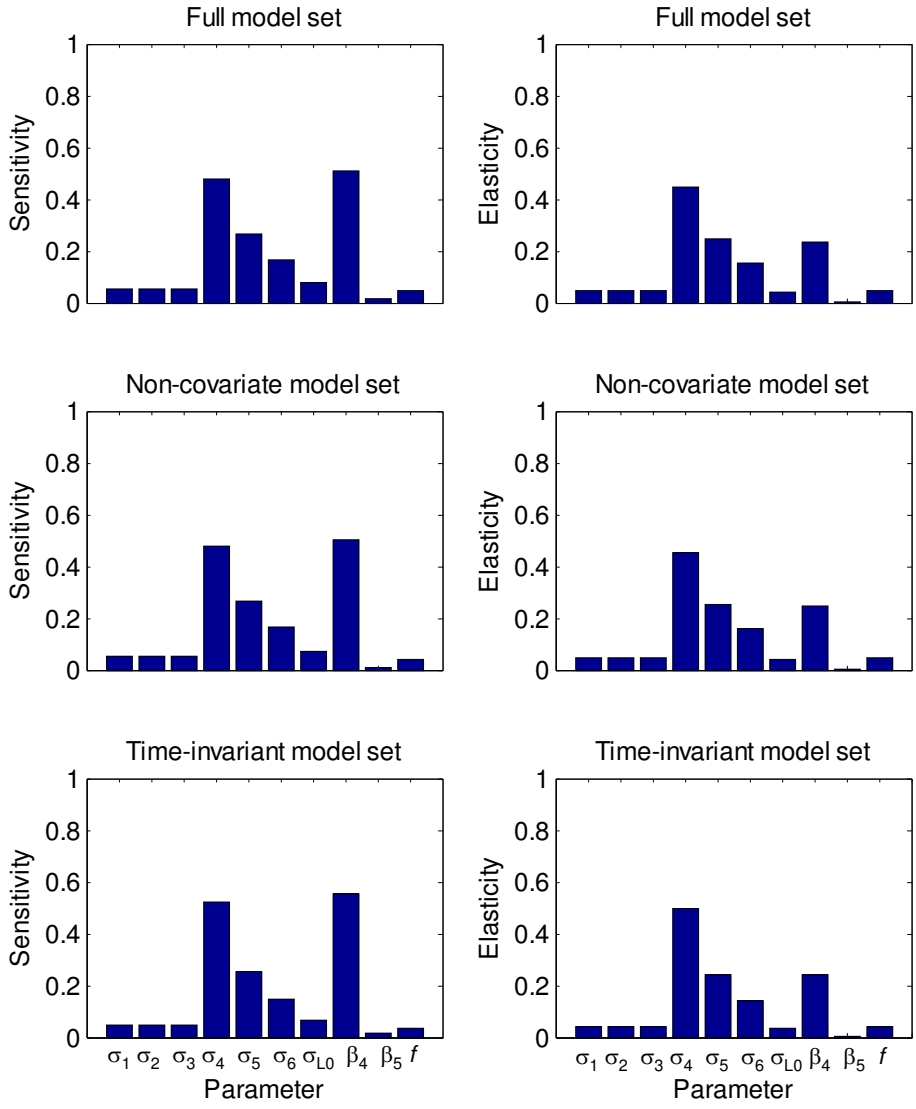

Figure A-2: Sensitivity (left column) and elasticity (right column) of population growth rate to parameter estimates from the full, non-covariate and time-invariant model sets for conditions in 2001.

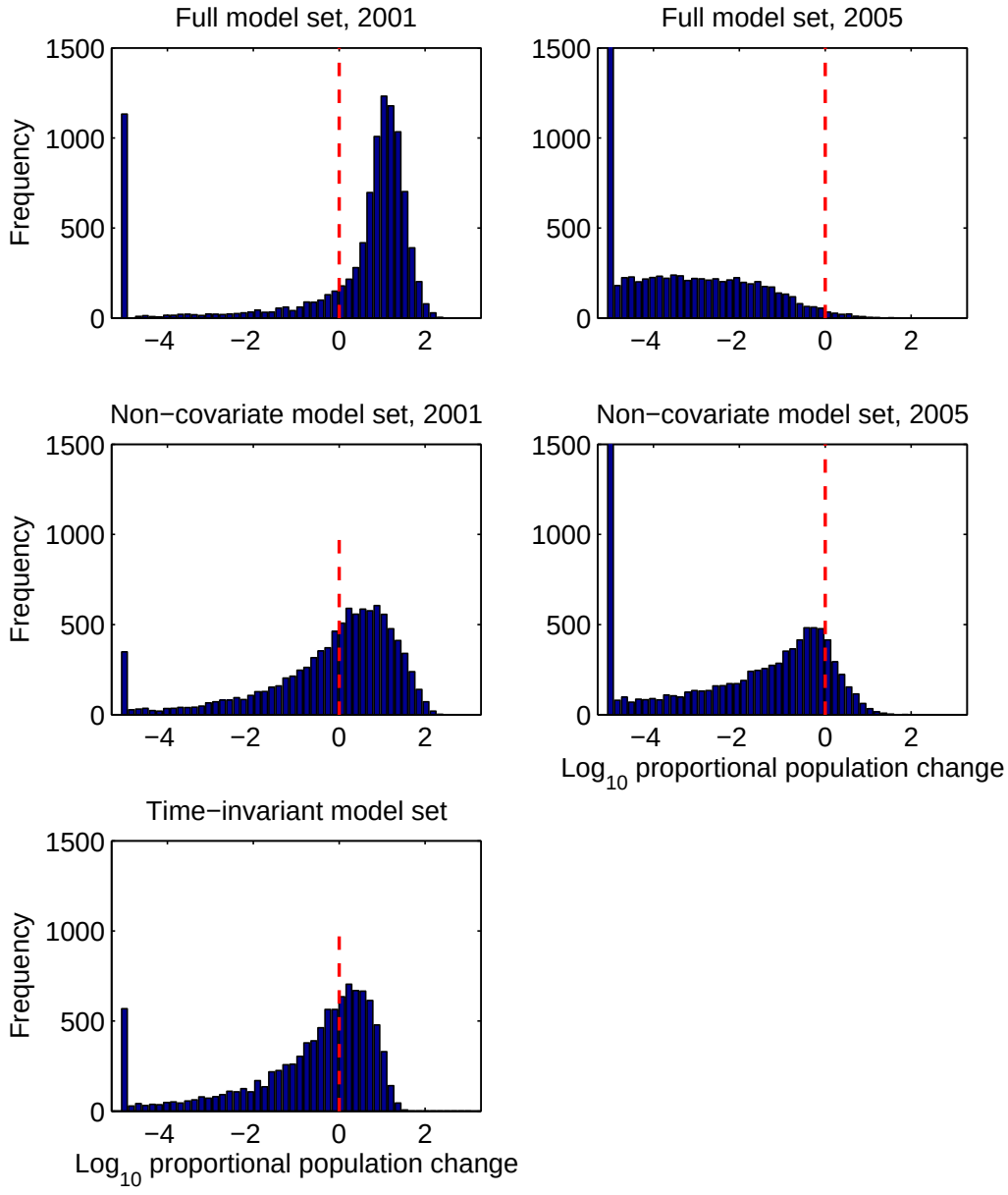

Figure A-3: Distribution of the log of population size at 45 years relative to the starting population size for parameter estimates from the full and non-covariate model sets in 2001 and 2005.

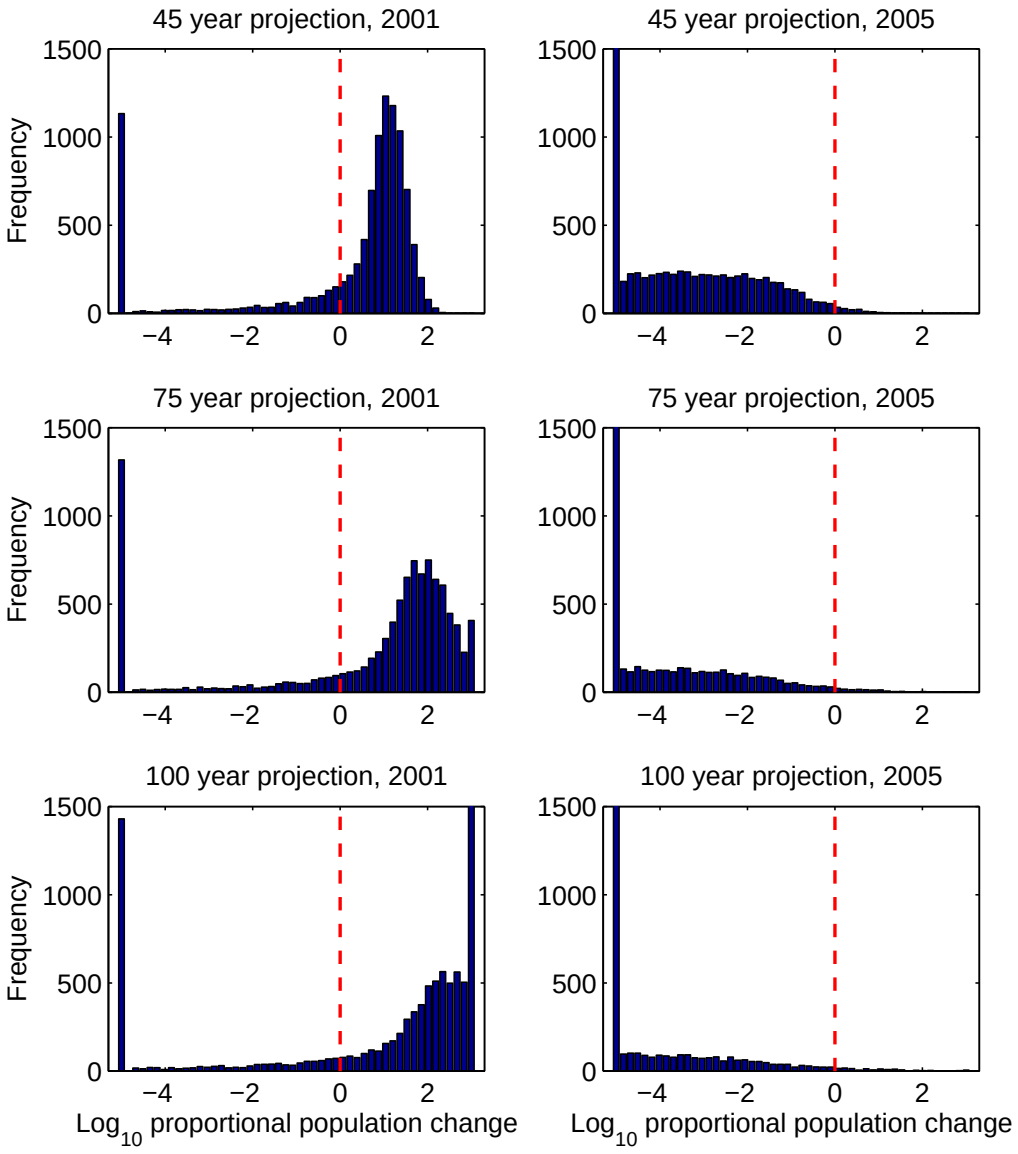

Figure A-4: Distribution of the log of population size at 45, 75 and 100 years relative to the starting population size for parameter estimates from the full model set in 2001 and 2005.

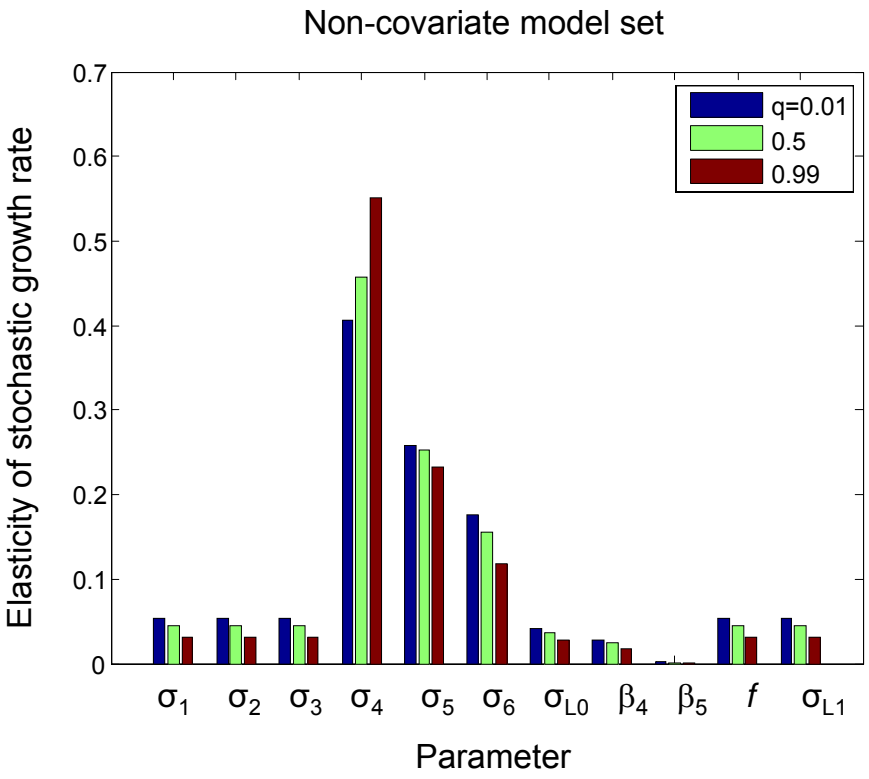

Figure A-5: Elasticity of the stochastic growth rate λ_s for three values of the probability q of bad ice conditions for parameter estimates from the non-covariate model set.

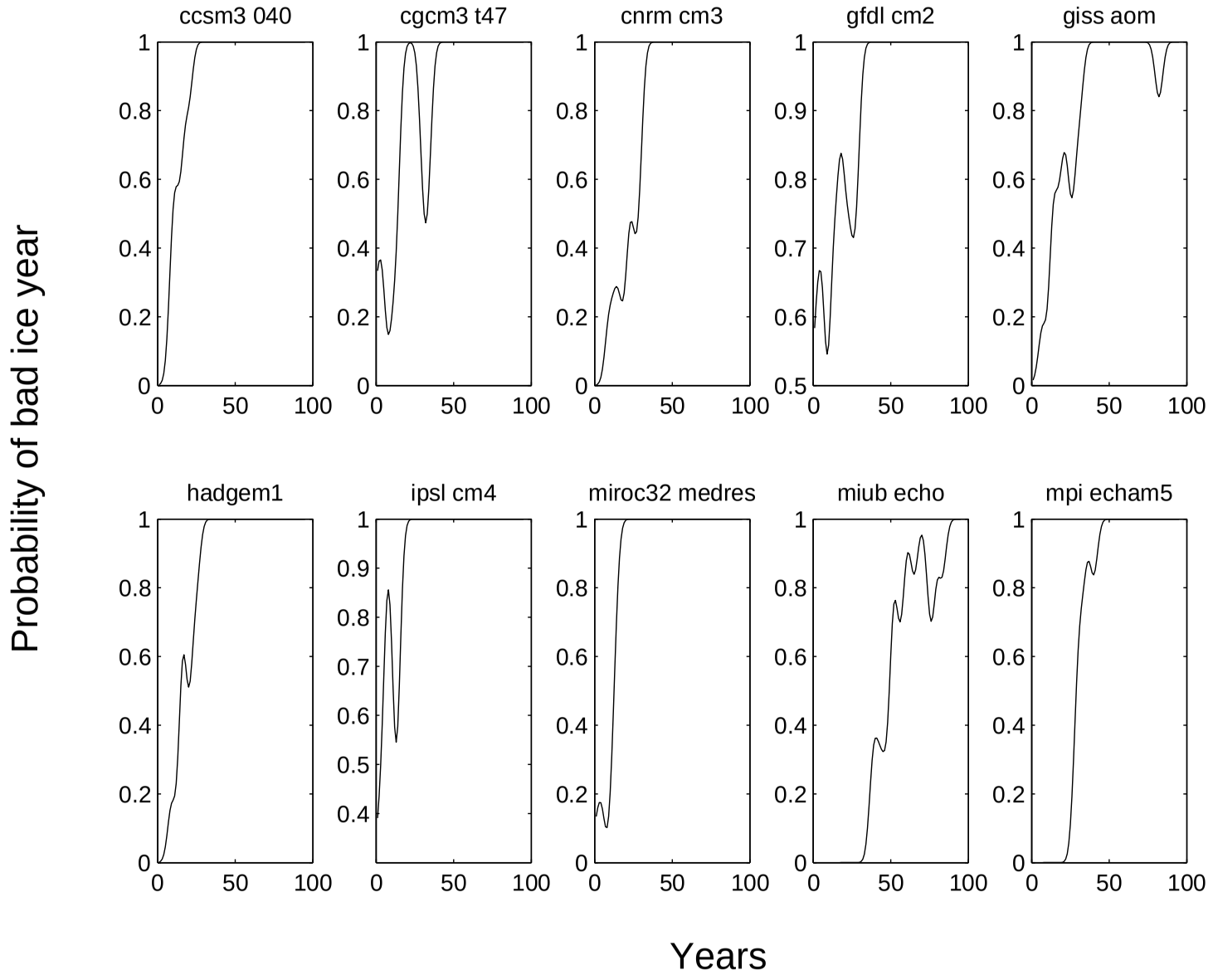

Figure A-6: Projected probability of bad ice years, from 2005–2100, from each of 10 GCM climate models.

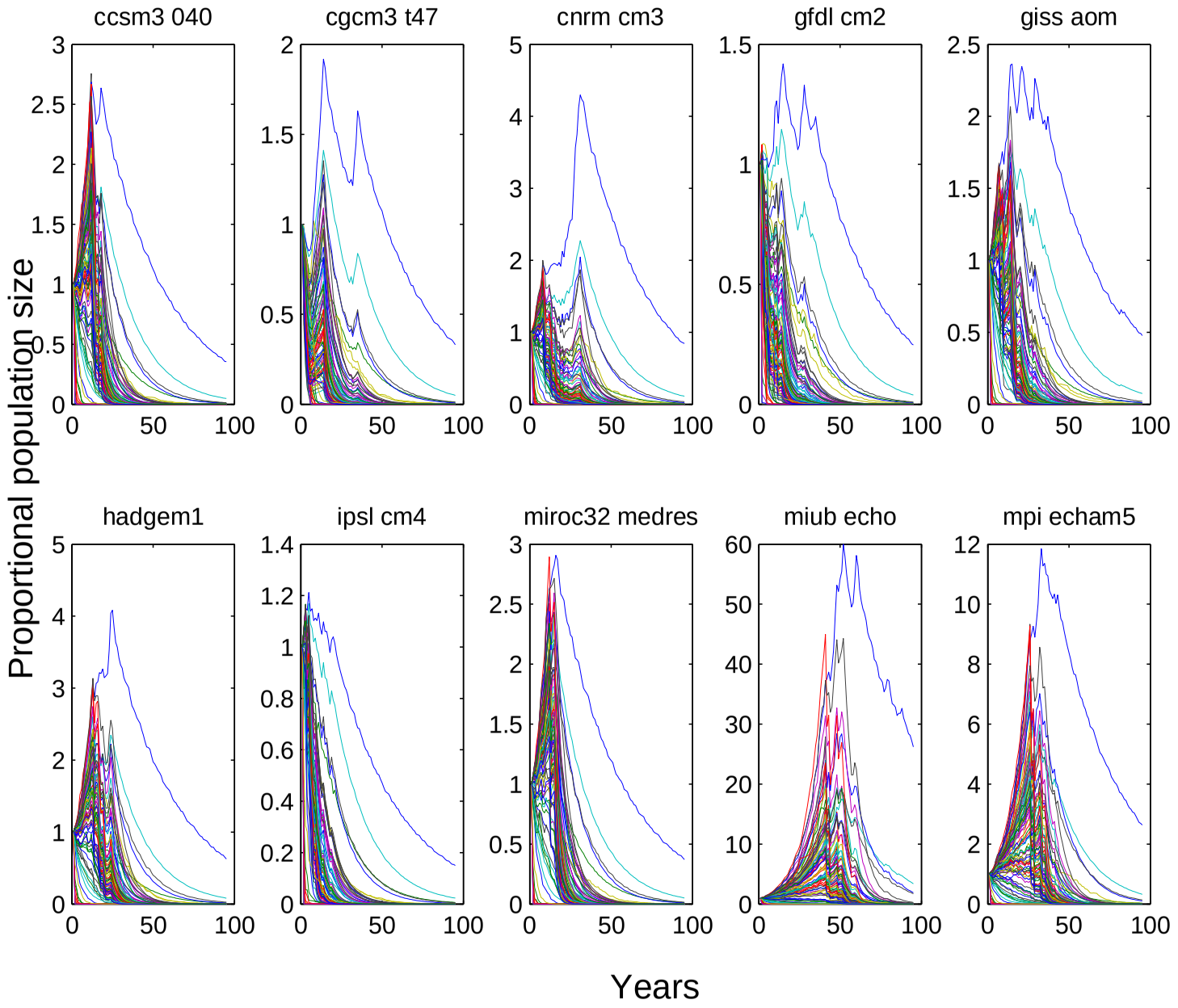

Figure A-7: Stochastic projection of total population size based on sea ice projections from 10 GCM climate models (see text for details). The multiple lines in each panel are a set of 50 bootstrap samples from the weighted models for the vital rates (full model set), applied to a single realization of the environment.

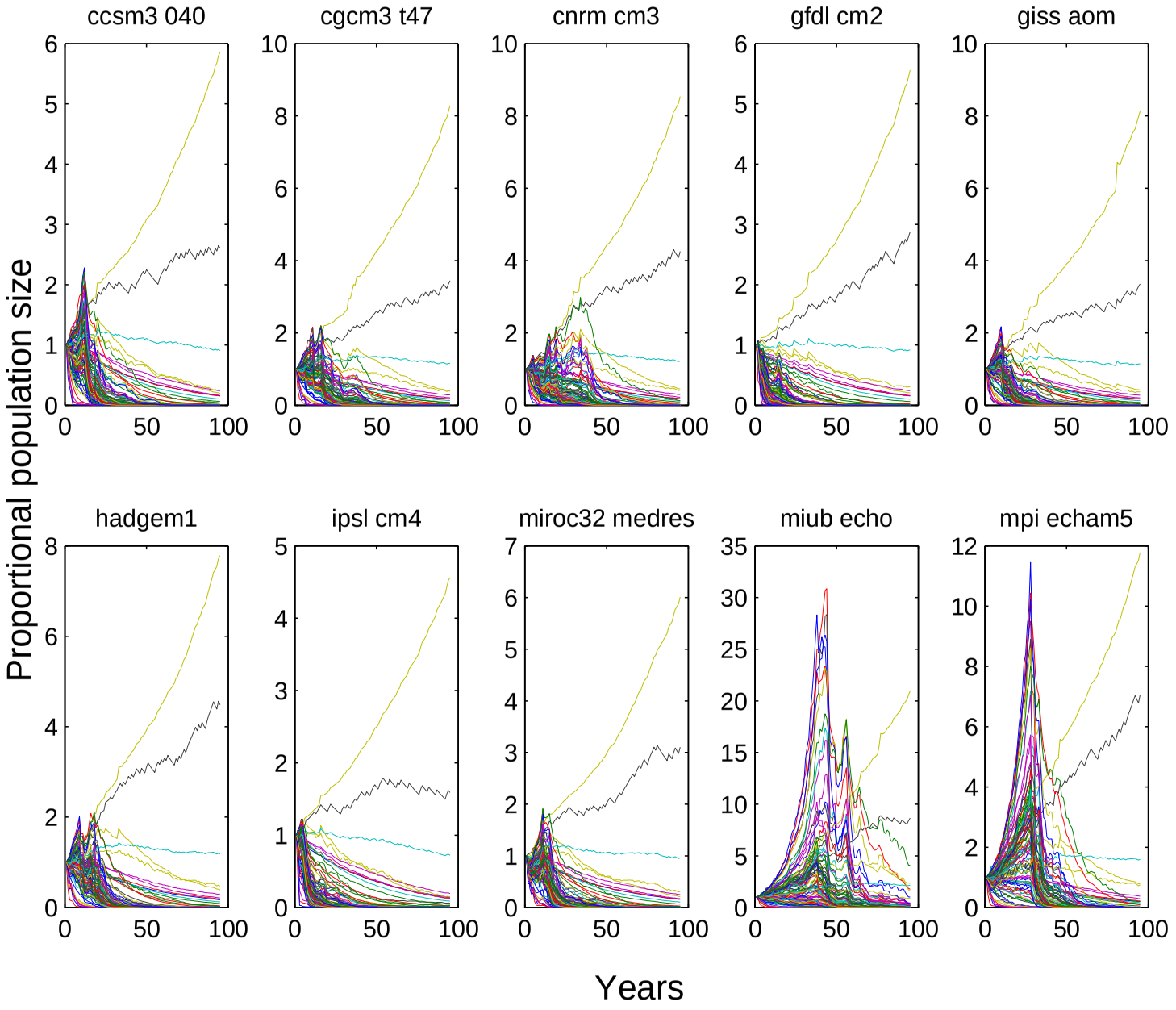

Figure A-8: Stochastic projection of total population size based on sea ice projections from 10 GCM climate models (see text for details). The multiple lines in each panel are a set of 50 bootstrap samples from the weighted models for the vital rates (non-covariate model set), applied to a single realization of the environment.